

Original Article

Neuroanatomical Distribution of Disease-Associated Prion Protein in Experimental Bovine Spongiform Encephalopathy in Cattle after Intracerebral Inoculation

Shigeo Fukuda¹, Sadao Onoe^{1**}, Satoshi Nikaido^{1***}, Kei Fujii¹,
Soichi Kageyama¹, Yoshifumi Iwamaru², Morikazu Imamura², Kentaro Masujin²,
Yuichi Matsuura², Yoshihisa Shimizu², Kazuo Kasai², Miyako Yoshioka³,
Yuichi Murayama², Shirou Mohri², Takashi Yokoyama², and Hiroyuki Okada^{2*}

¹Animal Research Center, Hokkaido Research Organization, Hokkaido 081-0038; and
²Prion Disease Research Center and ³Pathology and Pathophysiology Research Division,
National Institute of Animal Health, Ibaraki 305-0856, Japan

(Received September 2, 2011. Accepted November 17, 2011)

SUMMARY: The pathologic disease-associated prion protein (PrP^{Sc}) has been shown to be expressed in the central nervous system of Holstein cattle inoculated intracerebrally with 3 sources of classical bovine spongiform encephalopathy (BSE) isolates. Several regions of the brain and spinal cord were analyzed for PrP^{Sc} expression by immunohistochemical and Western blotting analyses. Animals euthanized at 10 months post-inoculation (mpi) showed PrP^{Sc} deposits in the brainstem and thalamus, but no vacuolation; this suggested that the BSE agent might exhibit area-dependent tropism in the brain. At 16 and 18 mpi, a small amount of vacuolation was detected in the brainstem and thalamus, but not in the cerebral cortices. At 20 to 24 mpi, when clinical symptoms were apparent, heavy PrP^{Sc} deposits were evident throughout the brain and spinal cord. The mean time to the appearance of clinical symptoms was 19.7 mpi, and the mean survival time was 22.7 mpi. These findings show that PrP^{Sc} accumulation was detected approximately 10 months before the clinical symptoms of BSE became apparent. In addition, the 3 sources of BSE prion induced no detectable differences in the clinical signs, incubation periods, neuroanatomical location of vacuoles, or distribution and pattern of PrP^{Sc} depositions in the brain.

INTRODUCTION

Bovine spongiform encephalopathy (BSE), a type of transmissible spongiform encephalopathy (TSE), is a fatal neurodegenerative disease affecting cattle. The disease was first identified in the United Kingdom (UK) in 1986 (1); subsequently, it spread to European, Asian, and North American countries. The first case of BSE in Japan was reported in September 2001 (2), and the most recent case, the 36th, was confirmed in January 2009. BSE is characterized by spongiform changes (3) and accumulation of the disease-associated prion protein (PrP^{Sc}) in the central nervous system (CNS) (4). PrP^{Sc} is commonly accepted as the pathological agent of BSE and is thought to be a post-translationally modified form of the host-encoded membrane glycoprotein (PrP^C) (5). PrP^{Sc} is the only known disease-specific marker (6,7).

The pathological agent of BSE is transmissible to different mammalian species. A variant form, i.e., the degenerative brain disease Creutzfeldt-Jakob Disease

(vCJD) has been reported in the UK and several other countries, and it is thought that this disease is caused by the consumption of BSE-contaminated beef products (8–11). Therefore, it is important to understand the pathogenesis of BSE in cattle in order to eliminate BSE-contaminated food from human food and thereby preserve public health.

The uniformity in the pathological features and biochemical profile of the proteinase K (PK)-resistant PrP^{Sc} (PrP^{res}) in BSE-affected cattle suggests that a single prion strain is responsible for BSE in these animals. Recently, variants of BSE (named atypical BSE) have been detected in cattle in Europe (12,13), North America (14,15), and Japan (16,17). Currently, atypical BSE cases are classified into 2 groups; those expressing PrP^{res} of lower (L-type BSE) molecular weight and those expressing PrP^{res} with higher (H-type BSE) molecular weight than the PrP^{res} of classical BSE (C-BSE) (18).

Our current knowledge of the pathogenesis of C-BSE in cattle is based on the examination of tissues obtained from orally infected cattle that have been euthanized at different stages of the disease. A mouse bioassay of infectivity showed that in cattle, the infection was limited to the brain, spinal cord, eyes, dorsal root ganglia, and distal ileum (19–21). Occasionally, infectivity has also been detected in the bone marrow and tonsils of experimentally infected cattle (22,23), and recent studies have shown that peripheral tissues other than the CNS may harbor PrP^{Sc} at the clinical stages of the disease (24,25). The distribution of PrP^{Sc} in the brain has been

*Corresponding author: Mailing address: Prion Disease Research Center, National Institute of Animal Health, 3-1-5 Kan-nondai, Tsukuba, Ibaraki 305-0856, Japan. Tel: +81-29-838-8333, E-mail: okadahi@affrc.go.jp

**Present address: Hokkaido Obihiro Meat Inspection Center, Hokkaido 080-2465, Japan.

***Present address: East Japan Breeding Farm, Zen-noh Livestock Co. Ltd., Iwate 020-0583, Japan.

mapped in both naturally occurring C-BSE and orally infected cattle (26–28). However, it would be of interesting to evaluate the relationship between the time of detection of PrP^{Sc} in the CNS and the clinical course of the disease. For this purpose, we used the intracerebral inoculation route to infect cattle with 3 different C-BSE strains—one isolated in Kanagawa, Japan (BSE/JP5); one, in Wakayama, Japan (BSE/JP6) (29); and one, in the UK (BSE/UK) (30). We then proceeded to measure the distribution of PrP^{Sc} in the CNS of the infected animals by immunohistochemical and Western blotting analyses.

MATERIALS AND METHODS

Ethical considerations: All experiments involving animals were approved by the Animal Ethical Committee and the Animal Care and Use Committee of both Hokkaido Animal Research Center and National Institute of Animal Health.

Inoculation of cattle with C-BSE agents: Brain homogenates (10% w/v) were prepared from the brainstems of 3 cattle: one had been naturally infected with C-BSE (BSE/UK) provided by the Veterinary Laboratory Agency, UK; one was infected with domestic Kanagawa-1 (BSE/JP5) at 80 months of age; and one was infected with domestic Wakayama (BSE/JP6) at 83 months of age (29,30). Sixteen female Holstein calves aged 3 months were used for this experiment ($n = 8$ for BSE/UK, $n = 4$ for BSE/JP5, and $n = 4$ for BSE/JP6) (Table 1). Each animal was inoculated in the right side of the midbrain and 1 mL of brain homogenate was withdrawn from the brain by using an 18-gauge 7-cm disposable needle (NIPRO, Osaka, Japan). Two uninfected cattle served as controls and were euthanized at 27 months of age.

Neuropathology: At necropsy, the brains and cerebella were removed and hemisected at the midline. Samples of various tissues were fixed in 10% neutral buffered formalin (pH 7.4) for 3 days at 37°C, including those of the left hemisphere and spinal cord at the levels of cervi-

cal (C8) and lumbar enlargement (L6). The contralateral side was frozen at -80°C for Western blotting analysis of PrP^{Res}. Coronal slices of the brain and various tissues were cut at 3–4 mm thickness and placed in plastic cassettes, which were immersed in 98% formic acid for 60 min at room temperature (RT) to reduce infectivity (31). The tissues were automatically processed through a graded series of alcohol to xylene and then paraffin-embedded (ETP-150C; Sakura Finetek Japan, Tokyo, Japan). Serial sections were cut at a thickness of 4 μm , mounted on silane-coated glass slides (New Silane II; Muto Pure Chemicals Co., Tokyo, Japan) and stained with hematoxylin and eosin or processed for immunohistochemistry, as described below. The distribution and extents of vacuolation in the brain were scored according to the method described by Simmons et al. (32). A vacuolation lesion profile was created by plotting the mean vacuolation score for each neuroanatomical area against the assigned code for that area.

PrP^{Sc} immunohistochemistry: For each animal, tissue samples were examined from at least 8 areas of the brain and 2 spinal cord levels: frontal lobe, striatum, thalamus, occipital lobe, midbrain, pons, medulla oblongata at the obex, and cerebellum, and the C8 and L6 levels of the spinal cord. The paraffin-embedded tissue sections were pretreated at RT for PrP^{Sc} antigen retrieval using a recently developed chemical method (33). Briefly, deparaffinized and rehydrated tissue sections were immersed in a bath of 98% formic acid for 5 min, incubated with 0.5% (w/v) potassium permanganate (in 0.1 M phosphate buffer, pH 7.0) for 10 min, and then washed in distilled water 3 times. The sections were soaked in 1% sodium disulfite for 2 min and then washed in distilled water. The slides were then immersed in a solution of 0.1% *N*-lauroylsarcosine, 75 mM sodium hydroxide, and 2% sodium chloride for 10 min. Next, the sections were washed in tap water for 5 min and then placed in an immunohistochemical autostainer (Dako Cytomation Autostainer Universal Staining System; Dako, Carpinteria, Calif., USA). They were then incubated sequentially with 1 $\mu\text{g}/\text{mL}$ anti-PrP primary monoclonal

Table 1. Summary of the clinical and pathological changes in cattle intracerebrally inoculated with the BSE agent

Case	Code	Inoculum	Time of clinical onset (mpi)	Clinical signs at onset	Terminal clinical signs	Time at necropsy (mpi)	Spongiform change	PrP ^{Sc} by IHC	PrP ^{Sc} by WB
1	0801	BSE/UK	None			3	–	–	–
2	9066	BSE/UK	None			10	–	+	+
3	9385	BSE/UK	None			12	–	+	+
4	3962	BSE/JP6	None			12	–	+	+
5	2601	BSE/UK	None			16	+	+	+
6	0886	BSE/UK	None			18	+	+	+
7	3955	BSE/JP6	None			19	+	+	+
8	4394	BSE/UK	18	gait abnormality	abnormal posture	20	+	+	+
9	3728	BSE/JP5	19	nervous	ataxia	21	+	+	+
10	5426	BSE/JP5	21	ataxia	ataxia	22	+	+	+
11	5523	BSE/JP6	19	nervous	ataxia	23	+	+	+
12	4437	BSE/UK	18	ataxia	ataxia	23	+	+	+
13	1479	BSE/JP5	20	gait abnormality	ataxia	23	+	+	+
14	5087	BSE/UK	19	gait abnormality	ataxia	24	+	+	+
15	3217	BSE/JP5	22	gait abnormality	ataxia	24	+	+	+
16	4612	BSE/JP6	22	abnormal posture	abnormal posture	24	+	+	+

BSE, bovine spongiform encephalopathy; mpi, months post-inoculation; IHC, immunohistochemistry; WB, Western blotting.

antibody (mAb) T1, goat anti-mouse Fab' universal immunoperoxidase polymer (Histofine SimpleStain MAX-PO (M); Nichirei, Tokyo, Japan), and 3-3' diaminobenzidine tetrachloride as the chromogen. The T1 primary mAb was raised against mouse PrP amino acid residues 121-231 and cross-reacts with bovine PrP (34). Finally, the sections were counterstained with hematoxylin. All the steps in the immunohistochemical staining procedure were carried out at RT.

Immunohistochemical PrP^{Sc} mapping and profiling:

For each animal, the topographical distribution of PrP^{Sc} deposition was mapped at 14 different areas of the CNS: frontal cortex, temporal cortex, parietal cortex, occipital cortex, striatum, hippocampus, thalamus, midbrain, pons, medulla oblongata at the obex, cerebellar cortex, cerebellar medulla, and spinal cord at C8 and L6 segments. The PrP^{Sc} were classified into 8 types, as previously published (27,35). Intracellular PrP^{Sc} were subdivided into intraneuronal and intraglial granular deposits. Reports indicate that the stellate-type of PrP^{Sc} immunolabeling in astrocytes differed from the intraglial-type labeling (27,35). Extracellular PrP^{Sc} depositions in the neuropil were classified as linear, perineuronal, fine particulate, coarse granular, and coalescing.

PrP^{Sc} accumulation was scored subjectively for intensity and extent on a scale from 0 to 4 (0, negative; 1, apparent at high magnification; 2, apparent at moderate magnification; 3, apparent at low magnification and moderate amounts of accumulation; and 4, large amounts of accumulation) (36,37); it was then topographically mapped to the different CNS areas mentioned above.

Western blotting: Tissue samples were obtained from 18 areas of the brain and spinal cord, as shown schematically in Fig. 1. The tissues were homogenized in a buffer containing 100 mM NaCl and 50 mM Tris-HCl (pH 7.6). The homogenate was mixed with an equal

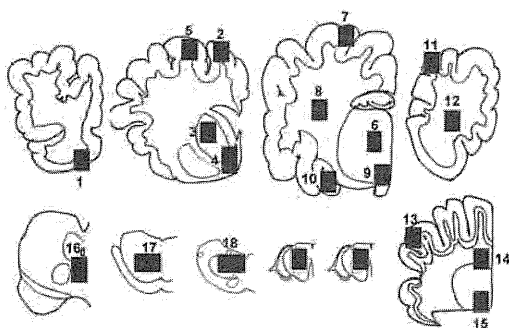


Fig. 1. The 18 areas of brain and spinal cord (black boxes) dissected for the Western blot analyses are schematically represented. They include 10 coronal slices of the brain and spinal cord at the levels of (from upper left) the frontal lobe, striatum, thalamus, occipital lobe, midbrain, pons, medulla oblongata at the obex, spinal cord at the cervical enlargement, spinal cord at the lumbar enlargement, and cerebellum. The brain regions are as follows: 1, frontal cortex; 2, parietal cortex; 3, caudate nucleus; 4, accumbens; 5, parietal cortex; 6, thalamus; 7, parietal cortex; 8, white matter at level of thalamus; 9, hypothalamus; 10, hippocampus; 11, occipital cortex; 12, occipital white matter; 13, cerebellar cortex; 14, cerebellar white matter; 15, cerebellar nucleus; 16, midbrain; 17, pons; and 18, obex.

volume of buffer containing 4% (w/v) Zwittergent 3-14 (Merck, Darmstadt, Germany), 1% (w/v) Sarkosyl, 100 mM NaCl, and 50 mM Tris-HCl (pH 7.6), and incubated with 0.25 mg collagenase, followed by incubation with PK (final concentration, 40 μ g/mL) at 37°C for 30 min. PK digestion was terminated by the addition of 2 mM Pefabloc (Roche Diagnostics, Basel, Switzerland). The sample was then mixed with 2-butanol:methanol (5:1) and centrifuged at 20,000 g for 10 min. The extracts were separated by 12% SDS-polyacrylamide gel electrophoresis (PAGE) and electroblotted onto a polyvinylidene fluoride (PVDF) membrane (Millipore, Billerica, Mass., USA). The blotted membrane was incubated with horseradish-conjugated anti-PrP mAb T2 (34) at RT for 60 min. Signals were developed with a chemiluminescent substrate (SuperSignal; Pierce Biotechnology, Rockford, Ill., USA).

RESULTS

Clinical signs: Of the 16 animals studied, 7 (Cases 1-7) showed no clinical signs of BSE even as late as 19 months post-inoculation (mpi) (Table 1). The remaining 9 animals (Cases 8-16) exhibited the initial clinical signs of disease between 18 and 22 mpi (19.7 ± 1.6 , mean \pm standard deviation); these signs included lowering of the head, heightened anxiety, and sensitivity to auditory stimuli. Within 2 to 3 months of the appearance of the initial clinical symptoms, the animals developed ataxia of the hind limbs, which progressed to difficulty in raising them without assistance. C-BSE-infected cattle were euthanized during this stage of the disease between 20 and 24 mpi (Table 1). There was no detectable difference in the clinical signs exhibited by animals inoculated with the 3 different C-BSE isolates.

Histopathology: The severity of vacuolation in the

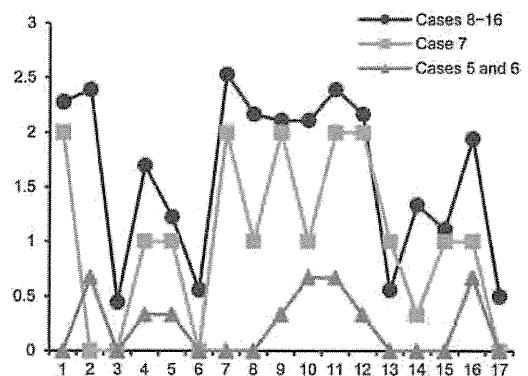


Fig. 2. Vacuolar lesion scores in BSE-challenged cattle at preclinical and clinical stages of the disease. Points from Cases 5 and 6 represent the means of 2 animals euthanized at the preclinical stage of disease at 16 and 18 mpi, respectively. Case 7 was euthanized at 19 mpi. Points for Cases 8-16 represent the mean score of 9 cases with clinical signs, euthanized between 20 and 24 mpi. Scores (y-axis) are plotted against the code numbers (x-axis) for anatomical areas as follows: 1, nucleus of the solitary tract; 2, nucleus of the spinal tract of the trigeminal nerve; 3, hypoglossal nucleus; 4, vestibular nuclear complex; 5, cochlear nucleus; 6, cerebellar vermis; 7, central gray matter; 8, rostral colliculus; 9, medial geniculate nucleus; 10, hypothalamus; 11, nucleus dorsomedialis thalami; 12, nucleus ventralis lateralis thalami; 13, frontal cortex; 14, accumbens; 15, caudate nucleus; 16, putamen; and 17, claustrum.

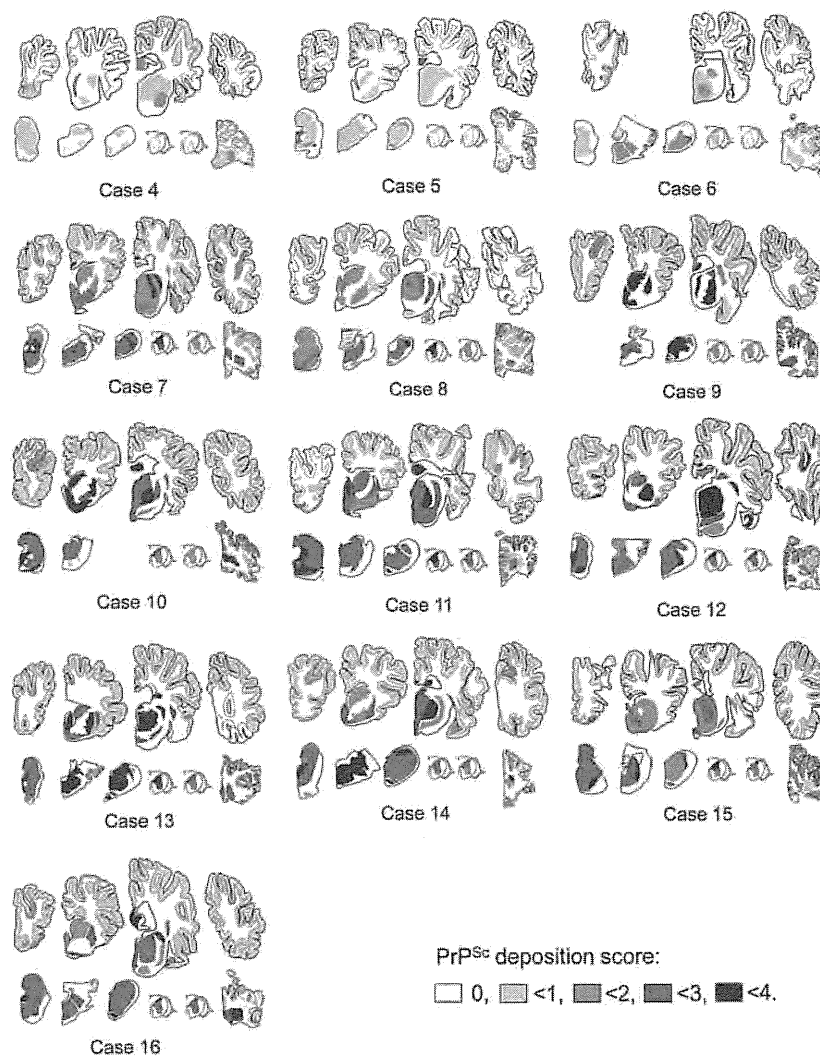


Fig. 3. Schematic representation of PrP^{Sc} in different brain areas of BSE-challenged cattle at preclinical (Cases 4–7) and clinical stages of the disease (Cases 8–16). The severity of PrP^{Sc} deposition is scored on a semi quantitative scale as 0 = no deposition, 1 = scanty, 2 = mild, 3 = moderate, and 4 = severe, with color gradation between white and black as indicated. Topographical brain areas schematically represent 10 coronal slices at the level of (from upper left to lower right): frontal lobe, striatum, thalamus, occipital lobe, midbrain, pons, medulla oblongata at the obex, spinal cord at the cervical enlargement, spinal cord at the lumbar enlargement, and cerebellum.

brain was scored as described in Methods, and the resulting lesion profiles are summarized in Fig. 2. Animals euthanized at 3, 10, and 12 mpi (Cases 1–4) had no vacuolar changes in any regions of the brain. Two cattle (Cases 5 and 6) were euthanized at 16 and 18 mpi, when clinical signs were absent, and they showed a few vacuoles in the neuropil of the thalamic nuclei, hypothalamus, pontine nuclei, nucleus of the spinal tract of trigeminal nerve, and putamen (Fig. 2). However, no vacuolation was detected in the cerebral and cerebellar cortices of these animals.

One animal (Case 7) showed no clinical signs of the disease and was determined to be at the preclinical stage of disease when euthanized at 19 mpi. This animal had a moderate number of vacuoles widely distributed throughout the brain (Fig. 2); vacuolation of the neuropil was evident in the thalamic nuclei, pons, and midbrain, and less frequently, in the cerebral cortices, especially in the caudal cerebrum.

Vacuolar changes of the brain were more frequent in the animals that exhibited clinical signs and were euthanized between 20 and 24 mpi (Cases 8–16) than in the 7 animals without clinical manifestations. The highest mean lesion scores were obtained for the thalamic nuclei and the neuropil of the central gray matter of the midbrain, and the lowest scores, for the caudal cerebral cortices and cerebellar cortex. Moreover, examination of the dorsal motor nucleus of the vagus nerve (DMNV) showed less characteristic vacuolar change. However, spongy change was much more severe and frequent in the trigeminal nucleus and solitary nucleus than in the other nuclei of the medulla oblongata at the obex level. Mild vacuolation was present in the neuropil of the gray matter in the spinal cords of all animals with clinical signs of the disease.

PrP^{Sc} immunohistochemistry: Figure 3 shows brain maps representing the topography and scoring of PrP^{Sc} at the frontal cortex level, striatum level, thalamus and

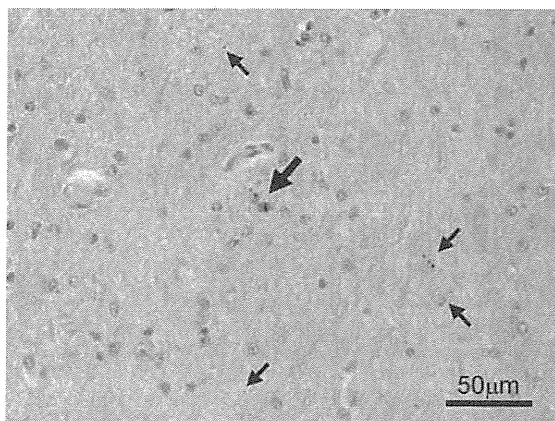


Fig. 4. Thalamus in Case 2. Intragial (large arrow) and particulate (small arrows) PrP^{Sc} immunolabeling is detected in the dorsolateral thalamic nucleus. Immunohistochemical labeling with mAb T1.

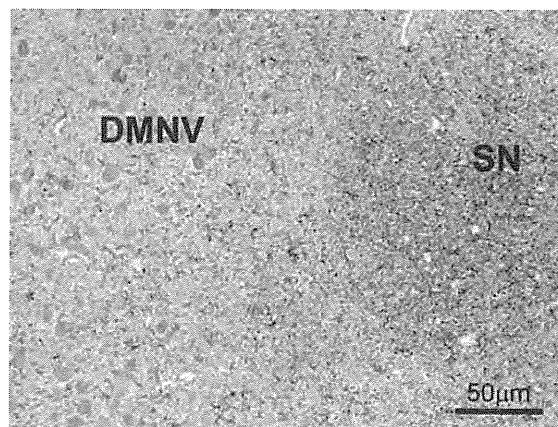


Fig. 5. Medulla oblongata at the obex level in Case 12. Particulate and granular PrP^{Sc} depositions are obvious in the neuropil of the nucleus of the solitary tract (SN). In contrast, PrP^{Sc} accumulation is sparse in the dorsal motor nucleus of the vagus nerve (DMNV). Immunohistochemical labeling with mAb T1 and hematoxylin counterstain.

parietal cortex level, occipital cortex level, midbrain, pons, obex, cerebellum, and spinal cords at the C8 and L6 segments of cattle.

The initial tissue lesion was detected as sparse PrP^{Sc} deposits in the neuronal perikarya and neuropil of gray matter, as neuritic-particulate or granular and linear types in the nuclei of thalamus (mostly ventricular nuclei), midbrain, pons, medulla oblongata (mostly spinal trigeminal nucleus), and septal accumbens of the animal euthanized at 10 mpi (Case 2; Fig. 4). Interestingly, the intraneuronal type of PrP^{Sc} deposit was more frequent than the other types. The neuritic-particulate or granular type of deposition showed neuronal process labeling. Perineuronal labeling was also detected, but less frequently. In the 2 animals euthanized at 12 mpi (Cases 3 and 4), small amounts of particulate or granular labeling in the neuronal cells and particulate or granular neuropil labeling were often present in the gray matter of the C8 and L6 segments of the spinal cord. However, no PrP^{Sc} deposit could be detected in the brain sections of the animal euthanized at 3 mpi (Case 1).

The animals (Cases 5 and 6) that had no clinical signs and were euthanized at 16 and 18 mpi exhibited moderate amounts of intraneuronal and intragial granular as well as particulate, linear, and coalescing neuropil labeling in the thalamus, midbrain, pons, medulla oblongata, cerebellar medulla, septal accumbens, and spinal cord. Minimal to slight PrP^{Sc} deposition was also present in the cerebral and cerebellar cortices, mostly in the frontal cortex.

Intraneuronal vacuoles were occasionally present in the brainstem and thalamic nuclei of the animal euthanized at 19 mpi (Case 7). PrP^{Sc} deposition was moderately localized in the brainstem, thalamic and septal nuclei, hypothalamus, cerebellar nuclei, and gray matter of the spinal cord, and was sparse in the rostral cerebral cortices and hippocampus. The labeling in the cerebral cortices of this animal was more apparent than that in the animals (Cases 5 and 6) euthanized at 16 and 18 mpi.

In general, the types and topographical distribution of PrP^{Sc} deposits were quite similar among the animals

that showed clinical signs of the disease (Cases 8–16; Fig. 3). The different types of immunolabeled PrP^{Sc}, i.e., the particulate or granular neuropil, intraneuronal, perineuronal, glial, linear, and coalescing types, were widely distributed throughout the brain. PrP^{Sc} immunolabeling was most pronounced in the brainstem, thalamus, the white matter of the cerebellum, and the gray matter of the spinal cord (Fig. 3). Small amounts of neuropil labeling were present in the DMNV at the level of the obex. In contrast, large amounts of PrP^{Sc} were evident in the nucleus of the solitary tract and the spinal tract nucleus of the trigeminal nerve (Fig. 5). Strong immunolabeling was conspicuous in both the cervical and lumbar segments of the spinal cord. Slight to moderate amounts of PrP^{Sc} deposits were dispersed in the cerebral and cerebellar cortices. The frontal cortex consistently showed the highest PrP^{Sc} deposition, while the lowest was noted in the occipital cortex. In the cerebellar cortex, PrP^{Sc} accumulation occurred in the granule cell layer, particularly just beneath the Purkinje cell layer.

Western blotting: A PrP^{res} signal was not detected in the brain extracts from the calf euthanized at 3 mpi (Case 1), but a small amount of PrP^{res} was detected in the brainstem and cerebellum of the animal killed at 10 mpi (Case 2; Fig. 6). The signal intensities of the extracts from different animals varied; for example, the signals obtained in Cases 4 and 7, in which the animals were killed at 12 and 19 mpi, respectively, were slightly stronger than those obtained in Cases 3 and 6, in which the animals were killed at similar time points (12 and 18 mpi, respectively). As seen in both Fig. 6 and Table 2, the spread of PrP^{res} throughout the brain and spinal cord correlated with the progression of the disease. The results of the Western blotting analyses are summarized in Table 2.

DISCUSSION

The goal of this study was to investigate the accumulation of PrP^{Sc} in the brain of cattle intracerebrally inoculated with the C-BSE prion agent. Although this

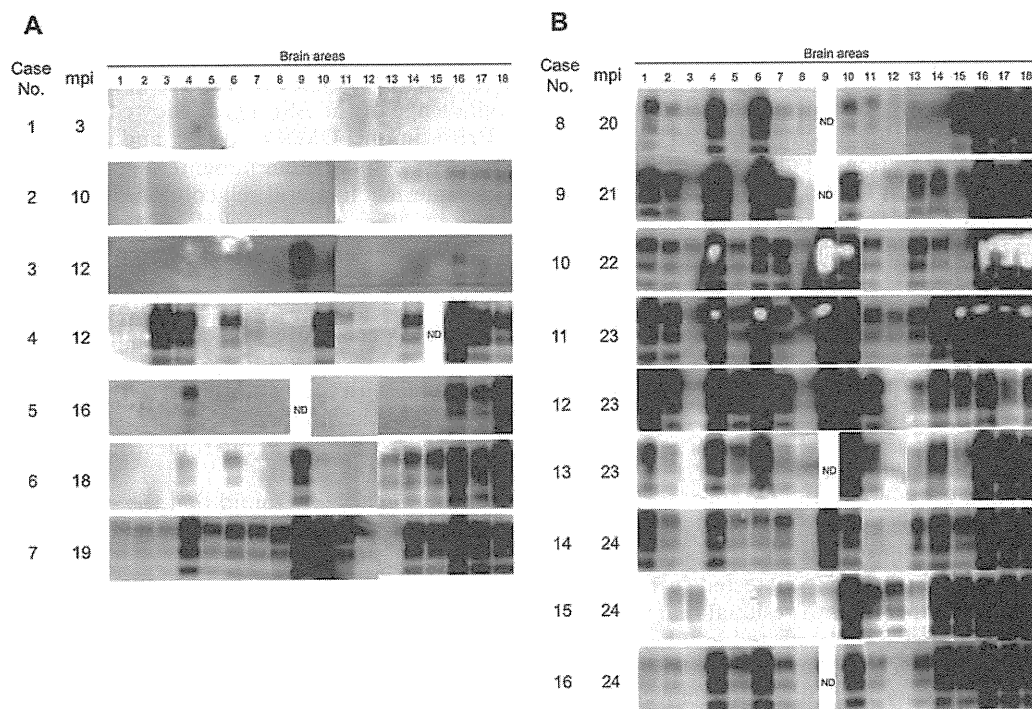


Fig. 6. Western blotting of PrP^{res} in the CNS extracts from animals at the preclinical (A) or clinical stages of disease (B). Lanes are numbered according to the 18 different CNS regions shown in Figure 1. Each lane was loaded with 20 mg of tissue. Western blots were probed with mAb T2 to detect PrP^{res}. ND, not done.

Table 2. Detection of PrP^{Sc} by Western blotting of CNS tissue samples

	Status	Preclinical							Clinical								
		Case no. Months post-inoculation	1 3	2 10	3 12	4 12	5 16	6 18	7 19	8 20	9 21	10 22	11 23	12 23	13 23	14 24	15 24
1*	Frontal cortex	-	-	-	-	-	-	+	++	++	++	++	++	++	++	-	+
2	Parietal cortex	-	-	-	-	-	-	+	++	++	++	++	++	++	++	+	+
3	Caudate nucleus	-	-	-	++	-	-	+	+	+	+	+	-	-	+	-	
4	Accumbens	-	-	-	++	++	+	++	++	++	++	++	++	++	++	-	++
5	Parietal cortex	-	-	-	-	-	-	++	+	++	++	++	++	++	++	-	++
6	Thalamus	-	-	-	++	-	+	++	++	++	++	++	++	++	++	-	++
7	Parietal cortex	-	-	-	-	-	-	++	+	++	++	++	++	++	++	+	++
8	White matter at level of thalamus	-	-	-	-	-	-	++	+	-	+	++	+	+	-	-	-
9	Hypothalamus	-	-	++	-	ND	++	++	ND	ND	++	++	++	ND	++	-	ND
10	Hippocampus	-	-	-	++	-	-	++	++	++	++	++	++	++	++	++	++
11	Occipital cortex	-	-	-	-	-	-	++	++	-	++	++	++	++	+	++	+
12	Occipital white matter	-	-	-	-	-	-	+	+	+	+	++	+	-	-	++	-
13	Cerebellar cortex	-	-	-	-	-	++	-	+	++	++	++	++	++	++	+	++
14	Cerebellar white matter	-	+	+	++	-	++	++	+	++	++	++	++	++	++	++	++
15	Cerebellar nucleus	-	+	-	ND	-	++	++	++	++	+	++	++	++	++	++	++
16	Midbrain	-	+	+	++	++	++	++	++	++	++	++	++	++	++	++	++
17	Pons	-	+	+	++	++	++	++	++	++	++	++	++	++	++	++	++
18	Obex	-	+	+	++	++	++	++	++	++	++	++	++	++	++	++	++
	Spinal cord (C7)	ND	ND	ND	ND	++	++	++	+	ND	++	++	++	++	++	++	++
	Spinal cord (L5)	ND	ND	ND	ND	++	++	++	++	ND	++	++	++	++	++	++	++

- , none; + , positive; ++ , strongly positive (compared to positive control of mouse scrapie-infected brain 1.6 µg tissue equivalent); ND, not done.

*Numbers correspond to the 18 different brain areas as shown in Fig. 1.

transmission route does not mimic the natural route of infection, which is most likely the ingestion of infectious material, intracerebral challenge seems to be the most efficient route for the synchronized induction of C-BSE in cattle. In line with this assumption, the incubation periods and disease durations of all the C-BSE-inoculated cattle were consistent with the findings of previous studies (38). In addition, although the number of study animals was small, the cattle inoculated with the 3 different C-BSE isolates did not differ in terms of the vacuolar lesion scores, the PrP^{Sc} topographical distribution, or the extent of PrP^{Sc} accumulation in the brain at the terminal disease stage. These results suggest that the 3 BSE strains used in this study may be identical and originate from a single infectious strain, which we denoted as the C-BSE prion.

We detected an early accumulation of PrP^{Sc} in the brainstem of infected animals; the reasons for this could be that the structure lies in the intracerebral inoculation path or because the brainstem is a target site for the C-BSE agent. Although the PrP^{Sc} detected in the brainstem could thus be attributed to residual material from the inoculation, no PrP^{Sc} was detected in the brainstem of the animal euthanized at 3 mpi (Case 1), either by Western blotting or by immunohistochemistry. This finding is consistent with a previous report of the experimental transmission of sheep scrapie (39). PrP^{Sc} might be widely distributed in a nonuniform manner from the inoculum point to other targeted brain areas, suggesting that the C-BSE prion had a strong regional tropism for the brainstem and thalamus (27). This possibility was not ruled out because we found that PrP^{Sc} was distributed throughout the brain and spinal cord, and not solely localized in the midbrain and cerebrum at the site of inoculation (40,41). In addition to the vacuolar lesion profiles, we found the topographical distribution of PrP^{Sc} in the brains of cattle with clinically evident disease to be consistent with that reported for cattle with naturally occurring BSE (27,29,35,42–45). The results described here also suggest that the accumulation and distribution of PrP^{Sc} in the brain correlated with the disease incubation period.

Although each C-BSE inoculum was prepared from the same brain region (brainstem) of infected cattle, we observed differences in the PrP^{res} signal intensity on Western blots between animals sacrificed at the same point after inoculation. For example, the intensity differed between Case 3 (BSE/UK) and Case 4 (BSE/JP6), wherein the animals were sacrificed at 12 mpi, and between Case 6 (BSE/UK) and Case 7 (BSE/JP6), wherein the animals were sacrificed at 18 and 19 mpi, respectively. These differences may be attributed to the low number of experimental animals used, variations in the infectivity titers of the inoculums, breeding conditions, or additional unknown factors associated with prion propagation in the brain.

The vacuolar lesion scores of symptomatic animals in this study were considerably higher than those of asymptomatic animals, and they were consistent with those previously described for BSE-affected cattle that had been naturally or experimentally infected (32,38,46). According to the current models of peripheral pathogenesis in orally induced TSEs, the BSE prion most probably reaches the medulla oblongata and then

spreads along the parasympathetic efferent fibers of the autonomic nerve system, i.e., the vagus nerves (47–49). In one study, cattle receiving a high-dose peroral challenge of the BSE agent showed initial deposition of PrP^{Sc} in the DMNV, celiac and mesenteric ganglion complex, and caudal mesenteric ganglion, as well as in the intermediolateral cell column of the spinal cord, but not in other areas, including the midbrain (26). The DMNV was also the first region of PrP^{Sc} deposition in the brain of cattle naturally affected by BSE (50) and those with experimental BSE induced by oral inoculation (26). Therefore, the discrepancy between the findings of our study and those reported for naturally occurring BSE with regard to the severity of vacuolar changes and PrP^{Sc} accumulation in the DMNV might be attributed to the different routes of infection in the individual studies.

In summary, we found that the earliest accumulation of PrP^{Sc} in intracerebrally inoculated cattle in the brainstem and thalamus occurred at 10 mpi, which was 10 months before the onset of clinical signs. PrP^{Sc} was widely distributed throughout the CNS during this preclinical period and accumulated at the target sites, mostly in the brainstem and thalamus. This study also indicated that clinical signs of the disease might appear after the appearance of vacuolar changes in the brain.

Acknowledgments We thank Drs. Tetsutaro Sata, Ken'ichi Hagiwara, and Yoshio Yamakawa, National Institute of Infectious Diseases, and the Expert Committee for BSE Diagnosis, Ministry of Health, Labour and Welfare of Japan, for providing the BSE isolates (BSE/JP5 and BSE/JP6), and Dr. Yuichi Tagawa, National Institute of Animal Health, for providing mAbs T1 and T2. Expert technical assistance was provided by Ms. Miyo Kakizaki, Tomoko Ishihara, Junko Endo, Mutsumi Sakurai, Megumi Hoshino, Ryoko Wakisaka, and the animal caretakers.

This work was supported by grants from the BSE and other Prion Disease Project of the Ministry of Agriculture, Forestry and Fisheries of Japan, and from the BSE research of the Ministry of Health, Labour and Welfare of Japan.

Conflict of interest None to declare.

REFERENCES

1. Wells, G.A., Scott, A.C., Johnson, C.T., et al. (1987): A novel progressive spongiform encephalopathy in cattle. *Vet. Rec.*, 121, 419–420.
2. Kimura, K.M., Haritani, M., Kubo, M., et al. (2002): Histopathological and immunohistochemical evaluation of the first case of BSE in Japan. *Vet. Rec.*, 151, 328–330.
3. Wells, G.A., Wilesmith, J.W. and McGill, I.S. (1991): Bovine spongiform encephalopathy: a neuropathological perspective. *Brain Pathol.*, 1, 69–78.
4. Prusiner, S.B., Bolton, D.C., Groth, D.F., et al. (1982): Further purification and characterization of scrapie prions. *Biochemistry*, 21, 6942–6950.
5. Prusiner, S.B. (1991): Molecular biology of prion diseases. *Science*, 252, 1515–1522.
6. Bolton, D.C., McKinley, M.P. and Prusiner, S.B. (1982): Identification of a protein that purifies with the scrapie prion. *Science*, 218, 1309–1311.
7. Prusiner, S.B. (1991): Molecular biology of prions causing infectious and genetic encephalopathies of humans as well as scrapie of sheep and BSE of cattle. *Dev. Biol. Stand.*, 75, 55–74.
8. Chazot, G., Broussolle, E., Lapras, C., et al. (1996): New variant of Creutzfeldt-Jakob disease in a 26-year-old French man. *Lancet*, 347, 1181.
9. Cousens, S.N., Vynnycky, E., Zeidler, M., et al. (1997): Predicting the CJD epidemic in humans. *Nature*, 385, 197–198.
10. Will, R.G., Alperovitch, A., Poser, S., et al. (1998): Descriptive

- epidemiology of Creutzfeldt-Jakob disease in six European countries, 1993-1995. EU Collaborative Study Group for CJD. *Ann. Neurol.*, 43, 763-767.
11. Will, R.G., Ironside, J.W., Zeidler, M., et al. (1996): A new variant of Creutzfeldt-Jakob disease in the UK. *Lancet*, 347, 921-925.
 12. Casalone, C., Zanusso, G., Acutis, P., et al. (2004): Identification of a second bovine amyloidotic spongiform encephalopathy: molecular similarities with sporadic Creutzfeldt-Jakob disease. *Proc. Natl. Acad. Sci. USA*, 101, 3065-3070.
 13. Biacabe, A.G., Laplanche, J.L., Ryder, S., et al. (2004): Distinct molecular phenotypes in bovine prion diseases. *EMBO Rep.*, 5, 110-115.
 14. Richt, J.A., Kunkle, R.A., Alt, D., et al. (2007): Identification and characterization of two bovine spongiform encephalopathy cases diagnosed in the United States. *J. Vet. Diagn. Invest.*, 19, 142-154.
 15. Dudas, S., Yang, J., Graham, C., et al. (2010): Molecular, biochemical and genetic characteristics of BSE in Canada. *PLoS ONE*, 5, e10638.
 16. Masujin, K., Shu, Y., Yamakawa, Y., et al. (2008): Biological and biochemical characterization of L-type-like bovine spongiform encephalopathy (BSE) detected in Japanese black beef cattle. *Prion*, 2, 123-128.
 17. Yamakawa, Y., Hagiwara, K., Nohtomi, K., et al. (2003): Atypical proteinase K-resistant prion protein (PrP^{res}) observed in an apparently healthy 23-month-old Holstein steer. *Jpn. J. Infect. Dis.*, 56, 221-222.
 18. Brown, P., McShane, L.M., Zanusso, G., et al. (2006): On the question of sporadic or atypical bovine spongiform encephalopathy and Creutzfeldt-Jakob disease. *Emerg. Infect. Dis.*, 12, 1816-1821.
 19. Wells, G.A., Dawson, M., Hawkins, S.A., et al. (1994): Infectivity in the ileum of cattle challenged orally with bovine spongiform encephalopathy. *Vet. Rec.*, 135, 40-41.
 20. Wells, G.A. H., Dawson, M., Hawkins, S.A.C., et al. (1996): Preliminary observations on the pathogenesis of experimental bovine spongiform encephalopathy. p. 28-44. 6th International Workshop on Bovine Spongiform Encephalopathy: the BSE Dilemma. Springer-Verlag, New York.
 21. Wells, G.A., Hawkins, S.A., Green, R.B., et al. (1998): Preliminary observations on the pathogenesis of experimental bovine spongiform encephalopathy (BSE): an update. *Vet. Rec.*, 142, 103-106.
 22. Hoffmann, C., Ziegler, U., Buschmann, A., et al. (2007): Prions spread via the autonomic nervous system from the gut to the central nervous system in cattle incubating bovine spongiform encephalopathy. *J. Gen. Virol.*, 88, 1048-1055.
 23. Wells, G.A., Hawkins, S.A., Green, R.B., et al. (1999): Limited detection of sternal bone marrow infectivity in the clinical phase of experimental bovine spongiform encephalopathy (BSE). *Vet. Rec.*, 144, 292-294.
 24. Wells, G.A., Spiropoulos, J., Hawkins, S.A., et al. (2005): Pathogenesis of experimental bovine spongiform encephalopathy: preclinical infectivity in tonsil and observations on the distribution of lingual tonsil in slaughtered cattle. *Vet. Rec.*, 156, 401-407.
 25. Buschmann, A. and Groschup, M.H. (2005): Highly bovine spongiform encephalopathy-sensitive transgenic mice confirm the essential restriction of infectivity to the nervous system in clinically diseased cattle. *J. Infect. Dis.*, 192, 934-942.
 26. Masujin, K., Matthews, D., Wells, G.A., et al. (2007): Prions in the peripheral nerves of bovine spongiform encephalopathy-affected cattle. *J. Gen. Virol.*, 88, 1850-1858.
 27. Vidal, E., Márquez, M., Tortosa, R., et al. (2006): Immunohistochemical approach to the pathogenesis of bovine spongiform encephalopathy in its early stages. *J. Virol. Methods*, 134, 15-29.
 28. Okada, H., Iwamaru, Y., Imamura, M., et al. (2011): Neuroanatomical distribution of disease-associated prion protein in cases of bovine spongiform encephalopathy detected by fallen stock surveillance in Japan. *J. Vet. Med. Sci.*, 73, 1465-1471.
 29. Iwata, N., Sato, Y., Higuchi, Y., et al. (2006): Distribution of PrP^{Sc} in cattle with bovine spongiform encephalopathy slaughtered at abattoirs in Japan. *Jpn. J. Infect. Dis.*, 59, 100-107.
 30. Yokoyama, T., Masujin, K., Yamakawa, Y., et al. (2007): Experimental transmission of two young and one suspended bovine spongiform encephalopathy (BSE) cases to bovinized transgenic mice. *Jpn. J. Infect. Dis.*, 60, 317-320.
 31. Taylor, D.M., Brown, J.M., Fernie, K., et al. (1997): The effect of formic acid on BSE and scrapie infectivity in fixed and unfixed brain-tissue. *Vet. Microbiol.*, 58, 167-174.
 32. Simmons, M.M., Harris, P., Jeffrey, M., et al. (1996): BSE in Great Britain: consistency of the neurohistopathological findings in two random annual samples of clinically suspect cases. *Vet. Rec.*, 138, 175-177.
 33. Bencsik, A.A., Debeer, S.O. and Baron, T.G. (2005): An alternative pretreatment procedure in animal transmissible spongiform encephalopathies diagnosis using PrP^{Sc} immunohistochemistry. *J. Histochem. Cytochem.*, 53, 1199-1202.
 34. Shimizu, Y., Kaku-Ushiki, Y., Iwamaru, Y., et al. (2010): A novel anti-prion protein monoclonal antibody and its single-chain fragment variable derivative with ability to inhibit abnormal prion protein accumulation in cultured cells. *Microbiol. Immunol.*, 4, 112-121.
 35. Debeer, S., Baron, T. and Bencsik, A. (2003): Neuropathological characterisation of French bovine spongiform encephalopathy cases. *Histochem. Cell. Biol.*, 120, 513-521.
 36. González, L., Martin, S., Begara-McGorum, I., et al. (2002): Effects of agent strain and host genotype on PrP accumulation in the brain of sheep naturally and experimentally affected with scrapie. *J. Comp. Pathol.*, 126, 17-29.
 37. González, L., Martin, S., Houston, F.E., et al. (2005): Phenotype of disease-associated PrP accumulation in the brain of bovine spongiform encephalopathy experimentally infected sheep. *J. Gen. Virol.*, 86, 827-838.
 38. Lombardi, G., Casalone, C., A, D. A., et al. (2008): Intraspecies transmission of BASE induces clinical dullness and amyotrophic changes. *PLoS Pathog.*, 4, e1000075.
 39. Hamir, A.N., Miller, J.M., Stack, M.J., et al. (2002): Failure to detect abnormal prion protein and scrapie-associated fibrils 6 wk after intracerebral inoculation of genetically susceptible sheep with scrapie agent. *Can. J. Vet. Res.*, 66, 289-294.
 40. Hamir, A.N., Kunkle, R.A., Cutlip, R.C., et al. (2005): Experimental transmission of chronic wasting disease agent from mule deer to cattle by the intracerebral route. *J. Vet. Diagn. Invest.*, 17, 276-281.
 41. Hamir, A.N., Miller, J.M., O'Rourke, K.I., et al. (2004): Transmission of transmissible mink encephalopathy to raccoons (*Procyon lotor*) by intracerebral inoculation. *J. Vet. Diagn. Invest.*, 16, 57-63.
 42. Orge, L., Simas, J.P., Fernandes, A.C., et al. (2000): Similarity of the lesion profile of BSE in Portuguese cattle to that described in British cattle. *Vet. Rec.*, 147, 486-488.
 43. Sisó, S., Ordóñez, M., Cerdón, I., et al. (2004): Distribution of PrP^{res} in the brains of BSE-affected cows detected by active surveillance in Catalonia, Spain. *Vet. Rec.*, 155, 524-525.
 44. Vidal, E., Márquez, M., Ordóñez, M., et al. (2005): Comparative study of the PrP^{BSE} distribution in brains from BSE field cases using rapid tests. *J. Virol. Methods*, 127, 24-32.
 45. Wells, G.A. and Wilesmith, J.W. (1995): The neuropathology and epidemiology of bovine spongiform encephalopathy. *Brain Pathol.*, 5, 91-103.
 46. Breslin, P., McElroy, M., Bassett, H., et al. (2006): Vacuolar lesion profile of BSE in the Republic of Ireland. *Vet. Rec.*, 159, 889-890.
 47. McBride, P.A. and Beekes, M. (1999): Pathological PrP is abundant in sympathetic and sensory ganglia of hamsters fed with scrapie. *Neurosci. Lett.*, 265, 135-138.
 48. McBride, P.A., Schulz-Schaeffer, W.J., Donaldson, M., et al. (2001): Early spread of scrapie from the gastrointestinal tract to the central nervous system involves autonomic fibers of the splanchnic and vagus nerves. *J. Virol.*, 75, 9320-9327.
 49. van Keulen, L.J., Schreuder, B.E., Vromans, M.E., et al. (2000): Pathogenesis of natural scrapie in sheep. *Arch. Virol. (Suppl.)*, 16, 57-71.
 50. Schulz-Schaeffer, W.J., Tschöke, S., Kranefuss, N., et al. (2000): The paraffin-embedded tissue blot detects PrP^{Sc} early in the incubation time in prion diseases. *Am. J. Pathol.*, 156, 51-56.



SHORT PAPER

Neuropathological Changes in Auditory Brainstem Nuclei in Cattle with Experimentally Induced Bovine Spongiform Encephalopathy

S. Fukuda^{*}, H. Okada[†], S. Arai[‡], T. Yokoyama[†] and S. Mohri[†]

^{*}Hokkaido Animal Research Center, Hokkaido Research Organization, Shintoku, Hokkaido 081-0038, [†]Prion Disease Research Center and [‡]Research Team for Production Diseases, National Institute of Animal Health, Kan-nondai 3-1-5, Tsukuba, Ibaraki 305-0856, Japan

Summary

Bovine spongiform encephalopathy (BSE) is characterized by the appearance of spongy lesions in the brain, particularly in the brainstem nuclei. This study evaluated the degenerative changes observed in the central auditory brainstem of BSE-challenged cattle. The neuropathological changes in the auditory brainstem nuclei were assessed by determining the severity of vacuolation and the presence of disease-associated prion protein (PrP^{Sc}). Sixteen female Holstein–Friesian calves, 2–4 months of age, were inoculated intracerebrally with BSE agent. BSE-challenged animals developed the characteristic clinical signs of BSE approximately 18 months post inoculation (mpi) and advanced neurological signs after 22 mpi. Before the appearance of clinical signs (i.e. at 3, 10, 12 and 16 mpi), vacuolar change was absent or mild and PrP^{Sc} deposition was minimal in the auditory brainstem nuclei. The two cattle sacrificed at 18 and 19 mpi had no clinical signs and showed mild vacuolar degeneration and moderate amounts of PrP^{Sc} accumulation in the auditory brainstem pathway. In the animals challenged with BSE agent that developed clinical signs (i.e. after 20 mpi), spongy changes were more prominent in the nucleus of the inferior colliculus compared with the other nuclei of the auditory brainstem and the medial geniculate body. Neuropathological changes characterized by spongy lesions accompanied by PrP^{Sc} accumulation in the auditory brainstem nuclei of BSE-infected cattle may be associated with hyperacusia.

© 2010 Elsevier Ltd. All rights reserved.

Keywords: auditory brainstem; BSE; cattle; prion

Transmissible spongiform encephalopathies (TSEs) are fatal neurodegenerative disorders that include bovine spongiform encephalopathy (BSE) in cattle, scrapie in sheep and goats, chronic wasting disease in deer and Creutzfeldt–Jacob disease in man. The key event in the pathogenesis of TSE is the conformational change of the normal host prion protein (PrP^C) into the abnormal, disease-associated form (PrP^{Sc}), which is thought to be the main, if not only, agent of TSE. BSE was first recognized in the UK in 1986 (Wells *et al.*, 1987) and was reported subsequently in several European countries and, more recently, in Japan, Canada and the USA. The histopathological features of BSE are spongy vacuolation of the neuropil

and vacuolation of neurons in the grey matter with mild astrogliosis and activation of microglia (Wells *et al.*, 1991).

It is difficult to determine the exact time of onset of BSE because of the non-specific nature of prodromal clinical signs. Typical clinical signs of BSE in cattle are changes in behaviour and locomotion and hypersensitivity to stimuli (Konold *et al.*, 2004). BSE-infected animals may be hypersensitive to touch, sound or light, but usually not to all of these types of stimuli. For example, cattle with BSE can become sensitive to noise (e.g. hand clapping or a metallic clank). The abnormality of brainstem auditory evoked potentials (BAEPs) in BSE-infected cattle has been reported to involve prolonged peak latency of wave III and V as well as the I–V interpeak

Correspondence to: H. Okada (e-mail: okadahi@affrc.go.jp).

0021-9975/\$ - see front matter
doi:10.1016/j.jcpa.2010.12.013

© 2010 Elsevier Ltd. All rights reserved.

Please cite this article in press as: Fukuda S *et al.* Neuropathological Changes in Auditory Brainstem Nuclei in Cattle with Experimentally Induced Bovine Spongiform Encephalopathy. *Journal of Comparative Pathology* (2011), doi:10.1016/j.jcpa.2010.12.013

latency (Arai *et al.*, 2009). The origin of wave III of the BAEP is the cochlear nucleus and superior olivary complex. The cochlear nucleus is the origin of the ascending central auditory pathway. Wave V arises in the inferior colliculus, the nucleus of which is the largest structure in the central auditory pathway and the focus for processing of both ascending and descending information. Little pathomorphological information, other than vacuolation in the cochlear nucleus described in a lesion profile, is available for the auditory brainstem of BSE-infected cattle (Simmons *et al.*, 1996; Breslin *et al.*, 2006). The aim of the present study was to investigate the neuropathological changes and PrP^{Sc} accumulation in the central auditory pathway of cattle exposed experimentally to BSE.

Sixteen female Holstein–Friesian calves, aged 2–4 months, were inoculated intracerebrally with 1 ml aliquots of 10% (w/v) brain homogenates prepared from three animals (from the UK and Japan) with naturally-occurring BSE. For negative controls, two calves received intracerebral inoculation of 10% brain homogenates of normal cattle.

At the time of necropsy examination, the left brain, including the brainstem and cerebellum, was fixed in 10% neutral buffered formalin (pH 7.4). Coronal slices of the formalin-fixed samples (4 mm) were immersed in 98% formic acid for 60 min to reduce infectivity, embedded in paraffin wax, sectioned (4 µm) and stained with haematoxylin and eosin (HE). The severity of vacuolation in the brain was scored according to the method of Simmons *et al.* (1996).

For immunohistochemistry (IHC), pretreatment for PrP^{Sc} antigen retrieval was conducted by a recently developed chemical method (Bencsik *et al.*, 2005). Briefly, dewaxed sections were immersed in 98% formic acid for 5 min, treated with 0.5% potassium permanganate (pH 7.0) for 10 min at room temperature and then washed thrice in distilled water. The sections were soaked in 1% sodium disulphite for 2 min and then washed once in distilled water. Sections were then immersed in a solution consisting of 0.1% *N*-laurylsarcosine, 75 mM sodium hydroxide and 2% sodium chloride for 10 min. After washing with water for 5 min, the sections were placed in an automated immunohistochemical processor (DakoCytomation Autostainer Universal Staining System; Dako, Carpinteria, California) and incubated with anti-PrP primary monoclonal antibody (mAb; T1), anti-mouse universal immunoperoxidase polymer (Nichirei Histofine Simple Stain MAX-PO (M); Nichirei, Tokyo, Japan) as the secondary antibody and 3,3'-diaminobenzidine tetrachloride as the chromogen. The primary mAb used in this study was raised against mouse PrP amino acid residues 121–231 and recognizes mouse PrP amino acid residues 137–143 (diluted at 1 µg/ml) (Shimizu *et al.*, 2010). Finally, sections were counterstained with haematoxylin.

The intensity and extent of each morphological type of PrP^{Sc} accumulation were scored subjectively from 0 to 4 (0, negative; 1, apparent at high magnification; 2, apparent at moderate magnification; 3, apparent at low magnification and moderate accumulation; 4, marked accumulation) as described by

Table 1
Individual animal data on clinical status, vacuolar lesion score and intensity of PrP^{Sc} accumulation

Case No.	Code No.	Inoculum	Post-inoculation period (months)	Clinical signs	Cochlear nucleus		Olivary nucleus		Lateral lemniscus		Inferior colliculus		Medial geniculate body		Auditory cortex	
					Lesion score	PrP ^{Sc} score	Lesion score	PrP ^{Sc} score	Lesion score	PrP ^{Sc} score	Lesion score	PrP ^{Sc} score	Lesion score	PrP ^{Sc} score	Lesion score	PrP ^{Sc} score
1	0801	BSE/UK	3	–	0	0	0	0	0	0	0	0	0	0	0	0
2	9066	BSE/UK	10	–	0	0	0	0	0	0	0	0	0	0.5	0	0
3	9385	BSE/UK	12	–	0	0	0	1	0	0	0	2	0	1	0	0
4	3962	BSE/JP5	12	–	0	1	0	1	0	0	0	1	0	1	0	0
5	2601	BSE/UK	16	–	0	2	0	2	0	0	1	2	0	2	0	0
6	0886	BSE/UK	18	–	2	3	1	3	0	0	1	1	0.5	1	0	0.5
7	3955	BSE/JP5	19	–	2	2.5	2	2.5	0	0	2	2	1	2.5	0	1
8	4394	BSE/UK	20	+	2	3	2	2	0	0.5	2	2	2	3	0	0.5
9	3728	BSE/JP6	21	+	NA	NA	NA	0	1	NA	NA	2	3.5	0	1	
10	5426	BSE/JP6	22	+	2	4	2	3	0	1	3	4	2	3	0	0.5
11	5523	BSE/JP5	23	+	2	3	2	3	0	1	4	4	2	3.5	0.5	1
12	4437	BSE/UK	23	+	3	3	3	3	0	1	4	3	2.5	3.5	0	0
13	1479	BSE/JP6	23	+	2	3	2	3	0	1	4	3	2.5	3	0.5	1
14	5087	BSE/UK	24	+	NA	NA	2	3	0	1	3	3.5	2	3.5	0.5	1
15	3321	BSE/JP6	24	+	2	3	2	3	0	1	2	3.5	2	3	0	0.5
16	4612	BSE/JP5	24	+	1	4	2	3.5	0	1	4	3	2.5	4	1	1

Clinical signs: +, positive; –, negative, NA, tissue not available.

González *et al.* (2002, 2005). Scored data from lesion profiles and immunohistochemical profiles were analyzed by one-way analysis of variance (ANOVA) using the statistical program Instat3 (GraphPad Software, San Diego, California) and were expressed as mean \pm standard deviation (SD).

BSE-infected cattle were killed at 3, 10, 12, 16, 18 and 19 months post inoculation (mpi) prior to developing signs of clinical disease (Table 1). One animal was killed at each time point, except at 12 months when two animals were killed. Nine animals, which demonstrated signs of clinical disease, were killed between 20 and 24 mpi. Two negative control animals were killed at 24 mpi. In the clinical cases of BSE-challenged cattle, initial clinical signs (e.g. abnormal posture and changes in locomotion) appeared between 18 and 20 mpi and advanced clinical signs (e.g. tremor and difficulties in rising) developed within 22–24 mpi. Clinical signs were not detected in the control cattle.

The four cattle that were killed at 3, 10 and 12 mpi had no vacuolar change in the brain, but some PrP^{Sc}

deposits were present in the brainstem nuclei and medial geniculate body of cattle killed at 10 or 12 mpi (Figs. 1 and 2). PrP^{Sc} was mostly detected in the perikarya (Fig. 2) and often in the neuropil of the grey matter of each auditory brainstem nucleus. In the animal killed at 16 mpi, minimal vacuolation was present in the nucleus of the inferior colliculus, but not in the cochlear nucleus, superior olivary complex or medial geniculate body (Fig. 3). Moreover, low to moderate amounts of PrP^{Sc} accumulated in the auditory brainstem nuclei (Fig. 4). In the two animals devoid of clinical signs that were killed at 18 and 19 mpi, mild vacuolar changes and moderate PrP^{Sc} accumulation were observed in the nuclei of the auditory brainstem and medial geniculate body (Figs. 1 and 2; Table 1).

All nine animals killed between 20 and 24 mpi had clinical signs of disease and spongy change was evident in the nucleus of the inferior colliculus. Prominent PrP^{Sc} accumulation was apparent in the auditory brainstem nuclei and medial geniculate body of nine animals (Figs. 3 and 4). Consistent

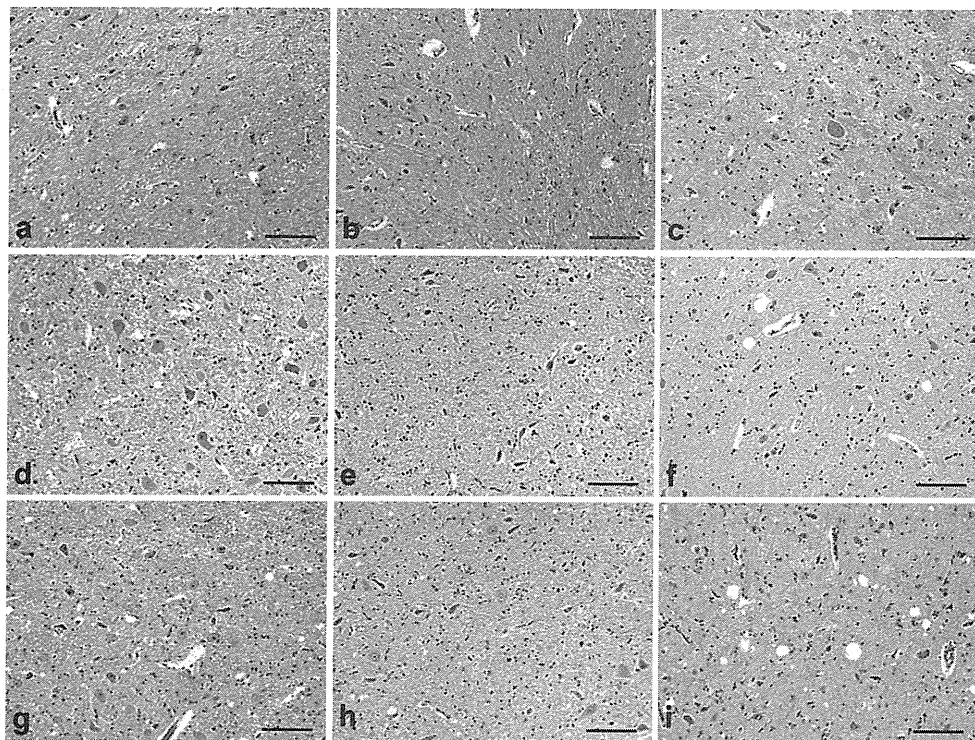


Fig. 1. Microscopical comparison of the auditory brainstem nuclei of BSE-challenged cattle killed at 12 (a–c), 19 (d–f) and 24 mpi (g–i). Images show the cochlear nucleus (a, d, g), nucleus of the trapezoid body (b, e, h) and nucleus of the inferior colliculus (c, f, i). No vacuolar changes were present at 12 mpi (a, b, c). Mild vacuolation was observed in the nucleus of the inferior colliculus at 19 mpi (f) and in the cochlear nucleus at 24 mpi (g). Moderate neuropil vacuolation was seen in the nucleus of the inferior colliculus at 24 mpi (i). HE. Bar, 100 μ m.

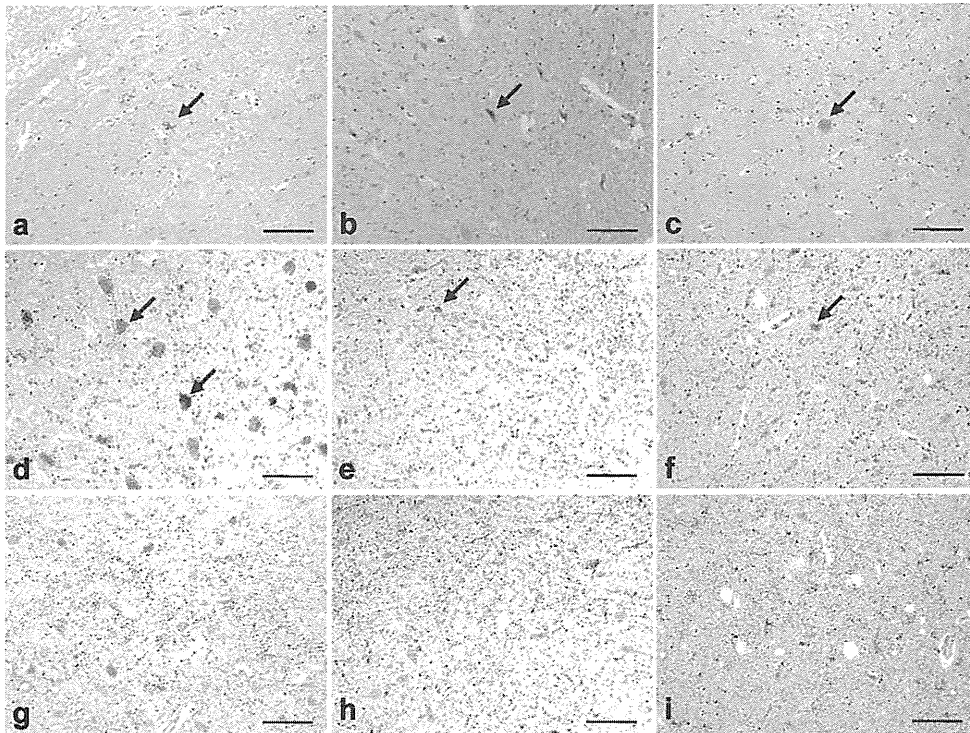


Fig. 2. Immunohistochemical comparison of PrP^{Sc} accumulation in the auditory brainstem nuclei of BSE-challenged cattle killed at 12 (a–c), 19 (d–f) and 24 mpi (g–i) using each semi-serial section shown in Fig. 1 (d–f). Images show the cochlear nucleus (a, d, g), nucleus of the trapezoid body (b, e, h) and nucleus of the inferior colliculus (c, f, i). Intraneuronal PrP^{Sc} accumulation (arrow) is observed in each auditory brainstem nucleus at 12 mpi (a–c). Intraneuronal (arrows) and granular accumulation of PrP^{Sc} is apparent in auditory brainstem nuclei at 19 (d–f) and 24 mpi (g–i). IHC. Bar, 100 μ m.

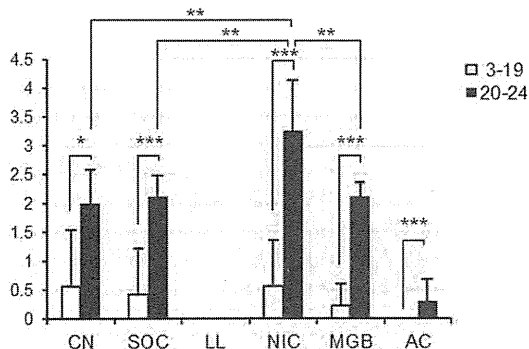


Fig. 3. Comparison of vacuolar lesion scores in the auditory brainstem nuclei of BSE-challenged cattle killed prior to 19 mpi (white rectangle) and after 20 mpi (black rectangle). Vacuolar change in the nucleus of the inferior colliculus after 20 mpi is significantly greater compared with changes in the cochlear nucleus, superior olivary complex and nucleus of medial geniculate body. CN, cochlear nucleus; SOC, superior olivary complex; LL, lateral lemniscus; NIC, nucleus of inferior colliculus; MGB, medial geniculate body; AC, auditory cortex. *** $P < 0.0001$; ** $P < 0.001$; * $P < 0.05$. All data are expressed as mean \pm SD.

PrP^{Sc} types in these areas were granular, punctate and intraneuronal. Other types of PrP^{Sc} deposition (e.g. linear, stellate, coalescing, intragial or perineuronal) were not evident in the nuclei of the auditory brainstem and medial geniculate body. The severity of vacuolation, as well as PrP^{Sc} accumulation in the nucleus of the inferior colliculus, of clinically-affected animals between 20 and 24 mpi was significantly higher than those of subclinical and preclinical animals prior to 19 mpi (Fig. 3). In animals with advanced neurological signs associated with BSE between 22 and 24 mpi, spongiosis and immunolabelled PrP^{Sc} deposits were evident in the nuclei of the auditory brainstem and medial geniculate body and were greatest in the nucleus of the inferior colliculus (Figs. 1 and 2; Table 1). The level of vacuolar change in the nucleus of the inferior colliculus at the clinical stage was significantly higher than levels in the cochlear nucleus, the superior olivary complex and the nucleus of medial geniculate body (Fig. 3), while the severity of PrP^{Sc} accumulation showed no significant difference among each nucleus at the same stage (Fig. 4). In addition, slight PrP^{Sc}

Changes in Auditory Brainstem Nuclei in BSE

5

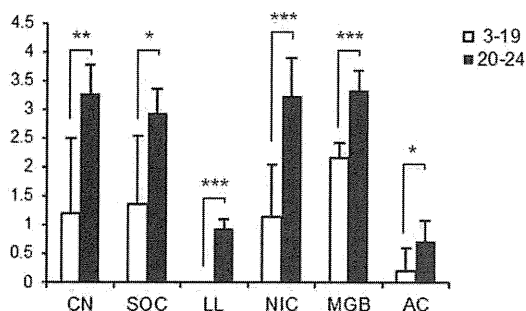


Fig. 4. Comparison of PrP^{Sc} immunolabelling in the auditory brainstem nuclei of BSE-challenged cattle killed prior to 19 mpi (white rectangle) and after 20 mpi (black rectangle). No significant differences in PrP^{Sc} accumulation were present in the auditory brainstem nuclei at the same stage. CN, cochlear nucleus; SOC, superior olivary complex; LL, lateral lemniscus; NIC, nucleus of inferior colliculus; MGB, medial geniculate body; AC, auditory cortex. *** $P < 0.0001$; ** $P < 0.001$; * $P < 0.05$. All data are expressed as mean \pm SD.

deposition was detected in the lateral lemniscus and auditory cortex.

Overall, typical spongiosis and PrP^{Sc} accumulation were mainly present in the neuropil of most brainstem nuclei of all BSE-challenged animals with clinical signs. However, intraneuronal vacuolation was minimal in most clinical cases. The various types of PrP^{Sc} deposition (Debeer *et al.*, 2003; Sisó *et al.*, 2004) were widely detected in the brain.

Cattle affected with BSE show progressive degeneration of the central nervous system (Wells *et al.*, 1991). Affected animals display many clinical signs that depend on the stage of the disease, which may worsen with time. It is difficult to diagnose BSE before clinical onset because early clinical signs of BSE are not always typical (Konold *et al.*, 2004). BSE-infected animals generally appear disturbed, anxious and nervous and are sensitive to loud noise or metallic sounds. These neurological signs usually appear at later stages of the disease.

In the nine animals showing clinical signs of BSE that were killed between 20 and 24 mpi, moderate vacuolar changes and abundant PrP^{Sc} accumulation were evident in all auditory brainstem nuclei. Clinical signs may appear after the presence of spongiform changes (Sisó *et al.*, 2004). Vacuolation was most prominent in the nucleus of the inferior colliculus compared with other auditory brainstem nuclei and the medial geniculate body. Lesion scoring of the cochlear nucleus has been reported to be very low compared with that of other brainstem nuclei (Simmons *et al.*, 1996; Breslin *et al.*, 2006). Topographical distribution of PrP^{Sc} deposits has been shown to correspond with vacuolar

lesions (Wells and Wilesmith, 1995), but PrP^{Sc} accumulation in some nuclei may not be accompanied by any vacuolation (Kimura *et al.*, 2002; Debeer *et al.*, 2003). Neuropathological appearance and topographical PrP^{Sc} immunolabelling in the brain of these two preclinical animals killed at 18 and 19 mpi were similar to those described previously in naturally-occurring cases of BSE (Kimura *et al.*, 2002; Debeer *et al.*, 2003; Sisó *et al.*, 2004).

To our knowledge, there is no appropriate tool currently available for ante-mortem diagnosis of BSE, and confirmation of the disease is only possible following post-mortem examination of brain tissue. In human prion diseases, the combination of auxiliary examinations based on an electroencephalogram and magnetic resonance imaging is used for clinical diagnosis (Cataldi *et al.*, 2000; Wieser *et al.*, 2006). In man, the audiometry of BAEP is a neurological test of auditory brainstem function in response to auditory stimuli, therefore BAEP changes may be accompanied by damage to the auditory pathways in the brain or auditory nerve indicative of underlying neuropathological alterations (Cascino *et al.*, 1988). Results of the present study suggest that spongy changes in the auditory brainstem nuclei, especially in the nucleus of the inferior colliculus of BSE-infected cattle, may be related to prolonged BAEP latency and reflect the dysfunction of auditory stimuli rather.

Acknowledgements

We thank Dr. Y. Tagawa for providing mAb T1 and Ms. J. Endo, M. Kakizaki, T. Ishihara, M. Sakurai and the animal caretakers for their expert technical assistance. This study was carried out under the guidelines of the Animal Ethical Committee and the Animal Care and Use Committee of the National Institute of Animal Health. This study was supported by grants for BSE and other prion disease control projects and the research project utilizing advanced technologies from the Ministry of Agriculture, Forestry and Fisheries of Japan.

References

- Arai S, Matsui Y, Fukuda S, Okada H, Onoe S (2009) Brainstem auditory evoked potentials in experimentally-induced bovine spongiform encephalopathy. *Research in Veterinary Science*, **87**, 111–114.
- Bencsik AA, Debeer SO, Baron TG (2005) An alternative pretreatment procedure in animal transmissible spongiform encephalopathies diagnosis using PrP^{Sc} immunohistochemistry. *Journal of Histochemistry and Cytochemistry*, **53**, 1199–1202.

- Breslin P, McElroy M, Bassett H, Markey B (2006) Vacuolar lesion profile of BSE in the Republic of Ireland. *Veterinary Record*, **159**, 889–890.
- Cascino GD, Ring SR, King PJ, Brown RH, Chiappa KH (1988) Evoked potentials in motor system diseases. *Neurology*, **38**, 231–238.
- Cataldi ML, Restivo O, Reggio E, Restivo DA, Reggio A (2000) Deafness: an unusual onset of genetic Creutzfeldt–Jakob disease. *Neurological Sciences*, **21**, 53–55.
- Debeer S, Baron T, Bencsik A (2003) Neuropathological characterisation of French bovine spongiform encephalopathy cases. *Histochemistry and Cell Biology*, **120**, 513–521.
- González L, Martin S, Begara-McGorum I, Hunter N, Houston F *et al.* (2002) Effects of agent strain and host genotype on PrP accumulation in the brain of sheep naturally and experimentally affected with scrapie. *Journal of Comparative Pathology*, **126**, 17–29.
- González L, Martin S, Houston FE, Hunter N, Reid HW *et al.* (2005) Phenotype of disease-associated PrP accumulation in the brain of bovine spongiform encephalopathy experimentally infected sheep. *Journal of General Virology*, **86**, 827–838.
- Kimura KM, Haritani M, Kubo M, Hayasaka S, Ikeda A (2002) Histopathological and immunohistochemical evaluation of the first case of BSE in Japan. *Veterinary Record*, **151**, 328–330.
- Konold T, Bone G, Ryder S, Hawkins SA, Courtin F *et al.* (2004) Clinical findings in 78 suspected cases of bovine spongiform encephalopathy in Great Britain. *Veterinary Record*, **155**, 659–666.
- Shimizu Y, Kaku-Ushiki Y, Iwamaru Y, Muramoto T, Kitamoto T *et al.* (2010) A novel anti-prion protein monoclonal antibody and its single-chain fragment variable derivative with ability to inhibit abnormal prion protein accumulation in cultured cells. *Microbiology and Immunology*, **54**, 112–121.
- Simmons MM, Harris P, Jeffrey M, Meek SC, Blamire IW *et al.* (1996) BSE in Great Britain: consistency of the neurohistopathological findings in two random annual samples of clinically suspect cases. *Veterinary Record*, **138**, 175–177.
- Sisó S, Ordóñez M, Cerdán I, Vidal E, Pumarola M (2004) Distribution of PrP(res) in the brains of BSE-affected cows detected by active surveillance in Catalonia, Spain. *Veterinary Record*, **155**, 524–525.
- Wells GA, Scott AC, Johnson CT, Gunning RF, Hancock RD *et al.* (1987) A novel progressive spongiform encephalopathy in cattle. *Veterinary Record*, **121**, 419–420.
- Wells GA, Wilesmith JW (1995) The neuropathology and epidemiology of bovine spongiform encephalopathy. *Brain Pathology*, **5**, 91–103.
- Wells GA, Wilesmith JW, McGill IS (1991) Bovine spongiform encephalopathy: a neuropathological perspective. *Brain Pathology*, **1**, 69–78.
- Wieser HG, Schindler K, Zumsteg D (2006) EEG in Creutzfeldt–Jakob disease. *Clinical Neurophysiology*, **117**, 935–951.

[Received, May 18th, 2010
Accepted, December 21st, 2010]

ORIGINAL ARTICLE

Sc237 hamster PrP^{Sc} and Sc237-derived mouse PrP^{Sc} generated by interspecies *in vitro* amplification exhibit distinct pathological and biochemical properties in tga20 transgenic mice

Miyako Yoshioka^{1,2}, Morikazu Imamura², Hiroyuki Okada², Noriko Shimozaki², Yuichi Murayama², Takashi Yokoyama² and Shirou Mohri²

¹Safety Research Team, and ²Prion Disease Research Center, National Institute of Animal Health, Tsukuba, Ibaraki, Japan

ABSTRACT

Prions are the infectious agents responsible for transmissible spongiform encephalopathy, and are primarily composed of the pathogenic form (PrP^{Sc}) of the host-encoded prion protein (PrP^C). Recent studies have revealed that protein misfolding cyclic amplification (PMCA), a highly sensitive method for PrP^{Sc} detection, can overcome the species barrier in several xenogeneic combinations of PrP^{Sc} seed and PrP^C substrate. Although these findings provide valuable insight into the origin and diversity of prions, the differences between PrP^{Sc} generated by interspecies PMCA and by *in vivo* cross-species transmission have not been described. This study investigated the histopathological and biochemical properties of PrP^{Sc} in the brains of tga20 transgenic mice inoculated with Sc237 hamster scrapie prion and PrP^{Sc} from mice inoculated with Sc237-derived mouse PrP^{Sc}, which had been generated by interspecies PMCA using Sc237 as seed and normal mouse brain homogenate as substrate. Tga20 mice overexpressing mouse PrP^C were susceptible to Sc237 after primary transmission. PrP^{Sc} in the brains of mice inoculated with Sc237-derived mouse PrP^{Sc} and in the brains of mice inoculated with Sc237 differed in their lesion profiles and accumulation patterns, Western blot profiles, and denaturant resistance. In addition, these PrP^{Sc} exhibited distinctive virulence profiles upon secondary passage. These results suggest that different *in vivo* and *in vitro* environments result in propagation of PrP^{Sc} with different biological properties.

Key words prion, protein misfolding cyclic amplification, species barrier, strain diversity.

Transmissible spongiform encephalopathies are fatal neurodegenerative disorders and include BSE, scrapie in sheep and goats, CWD in deer and elk, and CJD in humans (1). Prions are the infectious agents responsible for TSEs, which are characterized by PrP^{Sc} accumulation; PrP^{Sc} has a substantially different conformation than that of PrP^C (2). Different prion strains have been identified in most

species affected by TSE. This strain diversity can be explained by the inherent conformational flexibility of each type of PrP^{Sc}, which confers a specific disease phenotype in regard to characteristics such as incubation period, clinical symptoms, and neuropathological characteristics (3, 4). Prion strains are also characterized by the biochemical properties of PrP^{Sc}, including their glycosylation

Correspondence

Yuichi Murayama, Prion Disease Research Center, National Institute of Animal Health, 3-1-5 Kannondai, Tsukuba, Ibaraki, 305-0856 Japan.
Tel/fax: +81 298 38 8333; email: ymura@affrc.go.jp

Received 4 November 2010; revised 11 January 2011; accepted 5 February 2011.

List of Abbreviations: AP, alkaline phosphatase; BSE, bovine spongiform encephalopathy; CJD, Creutzfeldt-Jakob disease; CWD, chronic wasting disease; GdnHCl, guanidine hydrochloride; HE, hematoxylin and eosin; HRP, horseradish peroxidase; PK, proteinase K; PMCA, protein misfolding cyclic amplification; PNGase F, peptide: N-glycosidase F; PrP, prion protein; PrP^C, host-encoded cellular prion protein; PrP^{C-res}, proteinase K-resistant aggregated PrP^C; PrP^{Sc}, scrapie form of PrP^C; SEM, standard error of the mean; TSE, transmissible spongiform encephalopathy; vCJD, variant Creutzfeldt-Jakob disease; WB, Western blot.

profiles, electrophoretic mobility, and resistance to proteases and denaturants (5, 6). However, the mechanism by which a variety of PrP^{Sc} are generated from the same primary structure has not yet been elucidated.

Recent studies have reported that PMCA, a highly sensitive method for PrP^{Sc} detection (7–9), can overcome the species barrier in several xenogeneic combinations of PrP^{Sc} seed and PrP^C substrate, such as deer–ferret (10), deer–mouse (11), hamster–mouse, and mouse–hamster (12). Since BSE and vCJD are suspected to be attributable to cross-species transmission of prions (13), interspecies PMCA offers valuable insight into the origin and diversity of prions. However, a detailed comparison of PrP^{Sc} generated by interspecies PMCA and PrP^{Sc} accumulated in brains following cross-species transmission has not been undertaken because prion diseases are generally less transmissible to heterogeneous species. For example, a hamster scrapie prion strain, Sc237, has been described as non-infectious in wild-type mice because no clinical sign of disease was observed more than 735 days after intracerebral inoculation (14). This phenomenon is known as the “species barrier” (15), and is probably due to the species-specific physicochemical properties of prion proteins (16).

Although generation of a novel PrP^{Sc} with high infectivity can be reproduced in just a few days by interspecies PMCA (12), studies on the differences in PrP^{Sc} generated *in vivo* and *in vitro* are needed to examine whether PMCA is comparable to cross-species transmission of prion diseases *in vivo*. In this study, we demonstrated that tga20 transgenic mice overexpressing mouse PrP^C are susceptible to Sc237 following primary transmission. Therefore, we could compare PrP^{Sc} accumulated in the brains of mice inoculated with Sc237 and PrP^{Sc} from mice inoculated with Sc237-derived mouse PrP^{Sc} generated by interspecies PMCA using Sc237 as PrP^{Sc} seed and normal mouse brain homogenate as PrP^C substrate. The PrP^{Sc} that accumulated in the brains of these mice differed in their histopathological and biochemical properties, and exhibited different virulence patterns upon secondary transmission, suggesting that PrP^{Sc} with different biological properties propagate in a heterogeneous environment depending on whether they are produced *in vivo* or *in vitro*.

MATERIALS AND METHODS

All animal experiments were performed according to the guidelines of the National Institute of Animal Health.

PMCA

To avoid contamination, normal brain homogenates were prepared in a laboratory that had never contained infected materials. To compare the amplification efficien-

cies of PrP^{Sc} in wild-type mouse- and transgenic mouse-based amplifications, the brains of ICR mice, PrP^C-overexpressing tga20 transgenic mice (17), and PrP knock-out (PrP^{0/0}) mice were separately homogenized in 20% (w/v) PBS containing complete protease inhibitors (Roche Diagnostics, Mannheim, Germany). The homogenates were stored in small aliquots at –80°C. The homogenates were mixed with an equal volume of elution buffer (PBS containing 2% Triton X-100 and 8mM EDTA) and incubated at 4°C for 1 hr with continuous agitation. After centrifugation at 4500 g for 5 min, the supernatant of ICR brain homogenate was ready for use as a PrP^C substrate. The brain homogenates (10%) of PrP^{0/0} and tga20 mice were prepared as described above, and mixed in a 5:1 proportion of PrP^{0/0}:tga20. This mixture was also used as a PrP^C substrate.

Mouse-adapted scrapie strain Chandler was used as the PrP^{Sc} seed. The prion strain was propagated in ICR mice. The brains of mice in the terminal stage of disease were homogenized at a 10% concentration (w/v) in PBS. PMCA was carried out using a fully automatic cross-ultrasonic protein activating apparatus (Elestein 070-GOT, Elekon Science, Chiba, Japan) as reported previously (18). Amplification was performed by 40 cycles of sonication, in which a 3s pulse oscillation was repeated 5 times at 0.1s intervals, followed by incubation at 37°C for 1hr with gentle agitation (19).

Interspecies PMCA

PrP^C substrate prepared from ICR mice was used for interspecies PMCA. In addition, PrP^C substrate containing digitonin was prepared by adding digitonin (Nacalai Tesque, Kyoto, Japan) to a mixture of mouse brain homogenate and elution buffer at a final concentration of 0.05% prior to incubation and centrifugation. This PrP^C substrate was used for the first and second rounds of amplification.

A hamster-adapted scrapie prion strain, Sc237, was propagated in hamsters. When the animals had reached the terminal disease stage, they were killed and their brains pooled and homogenized in 10% (w/v) PBS containing 1% Triton X-100 and 4mM EDTA. After centrifugation at 4500 g for 5 min, the supernatant was used as the PrP^{Sc} seed. The Sc237 seeds were diluted 1:100 in ICR mouse PrP^C substrate containing digitonin (total volume, 100 μ L) in an electron-beam irradiated polystyrene tube. Amplification was performed by 40 cycles of sonication, in which a 3s pulse oscillation was repeated five times at 1s intervals, followed by incubation at 37°C for 1 hr with gentle agitation. After two cycles of 1:10 dilution of the PMCA product and subsequent amplification, the PrP^{Sc} signal on WBs was gradually attenuated. The pulse oscillation

interval was changed from 1.0 to 0.1s, and amplification was performed in the absence of digitonin after the second amplification round as reported previously (19). The PMCA products were diluted 1:10 in each of the second through eighth rounds of amplification, and 1:1 000–1:10 000 from the ninth through the 22nd round. The final dilution of the PrP^{Sc} seed was 10⁻³⁹ in the PMCA product of the 22nd amplification round. A negative control reaction (PrP^C substrate only) was performed simultaneously in the same manner.

Western blotting

Samples (10 μ L) from each round of amplification were mixed with 10 μ L of PK solution (100 μ g/mL) and incubated at 37°C for 1 hr. In some experiments, PK-digested samples were treated with PNGase F (New England BioLabs, Ipswich, MA, USA) to remove sugar chains on the PrP^{Sc} molecules, according to the manufacturer's instructions. The digested materials were mixed with 20 μ L of 2 \times SDS sample buffer and incubated at 100°C for 5 min. The samples were separated by SDS-PAGE and transferred onto a polyvinylidene fluoride membrane (Millipore, Bedford, MA, USA). After blocking, the membrane was incubated for 1 hr with HRP-conjugated T2 monoclonal antibody diluted to 1:10,000. The T2 antibody, which recognizes a discontinuous epitope in amino acid residues 132–156 in the mouse PrP sequence, reacts with both mouse and hamster PrP (20, 21). Anti-PrP monoclonal antibodies 4E10 (HRP conjugated, diluted to 1:10,000) and 3F4 (AP conjugated, diluted to 1:10,000) were also used. The 4E10 antibody recognizes an epitope in amino acid residues 147–158 (RYYRENMRYYPN) of the mouse PrP sequence (22), but does not react with hamster PrP. The 3F4 antibody recognizes an epitope in amino acid residues 110–113 (MKHM) of the hamster PrP sequence (23), but does not react with mouse PrP. After washing, the blotted membrane was developed using Immobilon Western chemiluminescent HRP or AP substrate (Millipore), according to the manufacturer's instructions. Chemiluminescence was analyzed with the Light Capture system (Atto, Tokyo, Japan).

Cross-species transmission of scrapie PrP^{Sc}

The 10% homogenate of Sc237-infected hamster brains was injected intracerebrally (20 μ L per mouse) into five tga20 transgenic and five Tg52NSE transgenic mice (24), which overexpress mouse PrP^C and hamster PrP^C, respectively. The PMCA product obtained in the 22nd round (R22) of amplification was diluted 1:10 and injected intracerebrally into five tga20 and five Tg52NSE mice. Densitometric analysis of WBs revealed that the PrP^{Sc} signal intensity in the PMCA product was approximately one-

eighth of that in a 1% homogenate of Sc237-infected hamster brain. The 10% homogenate of Sc237-infected brains was therefore diluted by 1:800 for injection into the control mice. Animals at the terminal stage of disease were killed and the right hemisphere of the brain stored at -80°C for biochemical analysis. For secondary transmission, brain homogenates (10%) of the Sc237-infected (Sc237/tga #1) and PMCA product-inoculated mice (PMCA/tga #1) were injected intracerebrally (20 μ L per mouse) into four and five tga20 transgenic mice, respectively.

Biochemical characterization of scrapie PrP^{Sc} that accumulated in the brains of tga20 mice

Resistance to PK digestion and GdnHCl denaturation were examined in the PrP^{Sc} that accumulated in the brains of tga20 mice inoculated with Sc237 and PrP^{Sc} from the mice inoculated with the R22 PMCA product. To examine PK sensitivity, 10% brain homogenates of Sc237- and PMCA product-inoculated mice were digested with various concentrations of PK (0.05–5 mg/mL) at 37 °C for 1 hr. The digested materials were immediately mixed with an equal volume of 2 \times SDS sample buffer and incubated at 100°C for 5 min. The samples were analyzed by WB in three independent experiments. The average intensity of the PrP^{Sc} signal in each sample was expressed as the percentage of that in the sample digested with 0.05 mg/mL PK. The results were analyzed by one-way ANOVA and Tukey's multiple comparison test. The PK₅₀ value, which is the concentration of PK needed to reduce the signal intensity by half, was estimated from an approximate curve calculated with the experimental data.

To perform the guanidine denaturation assay, the 10% homogenate of Sc237- and PMCA product-inoculated brains was incubated with agitation at room temperature for 2 hr in various concentrations of GdnHCl ranging from 0 to 4.0 M. The samples were incubated with agitation at 4°C for 30 min in the presence of 10% Sarkosyl, and centrifuged at 100,000 *g* for 1 hr in a TL-100 ultracentrifuge (Beckman Coulter, Brea, CA, USA). The pellets were dissolved directly in a PK solution (0.05 mg/mL) and incubated at 37°C for 1 hr. The samples were analyzed by WB in three independent experiments. The average intensity of the PrP^{Sc} signal in each sample was expressed as a percentage of that in the sample prepared without GdnHCl. The results were statistically analyzed as described above. The GdnHCl₅₀ value, which is the concentration of GdnHCl needed to reduce the signal intensity by half, was estimated from an approximate curve calculated from the experimental data.

Histopathological analysis

The left hemispheres of the brains were fixed in 10% buffered formalin for neuropathological analysis.

Coronal slices of the brains were immersed in 98% formic acid to reduce infectivity and embedded in paraffin wax. Sections (4 μm) were cut and stained with HE. The lesion profile was determined by examination of the HE-stained sections and scoring the vacuolar changes in nine standard grey matter areas (25).

For PrP^{Sc} immunohistochemistry, sections were pre-treated with 3% H₂O₂ for 10 min at room temperature, and incubated with 10 $\mu\text{g}/\text{mL}$ PK in PBS containing 0.1% Triton-X for 10 min, followed by 10 min incubation in 150 mM sodium hydroxide at 60°C. PrP^{Sc} was detected in brain sections using anti-PrP monoclonal antibody SAF84 (SPI-Bio, Montigny le Bretonneux, France). The sections were incubated with SAF84 antibody at a concentration of 1 $\mu\text{g}/\text{mL}$ for 60 min. Immunoreactions were developed using anti-mouse universal immuno-peroxidase polymer (Nichirei Histofine Simple Stain MAX-PO (M), Nichirei, Tokyo, Japan) as the secondary antibody, and 3–3'-diaminobenzidine tetrachloride as the chromogen with a Dako Cytomation Autostainer Universal Staining System (Dako, Carpinteria, CA, USA).

RESULTS

Amplification efficiencies of mouse PrP^{Sc} in ICR- and tga20-based amplifications

We compared the amplification efficiencies of Chandler PrP^{Sc} using ICR and tga20 brain homogenates as PrP^C substrates. For tga20-based amplification, it was necessary to dilute tga20 brain homogenate with PrP^{0/0} brain homogenate to obtain good amplification. Otherwise, the amplified PrP^{Sc} signal was indistinguishable from high background signals from protease-undigested PrP molecules (data not shown). Homogenates (10%) of Chandler-infected brain were diluted 1:100–1:100,000 with each of the PrP^C substrates, and one round of PMCA was performed (Fig. 1). A PrP^{Sc} signal was detected in duplicate samples of the 10⁻⁵ dilution samples in both ICR- and tga20-based amplifications, and WB profiles of amplified PrP^{Sc} from both amplifications were very similar. These observations suggest that wild-type PrP^C and diluted transgenic PrP^C have similar PrP^{Sc} amplification capabilities to Chandler strains *in vitro*. In the present study, ICR brain homogenate served as the PrP^C substrate for convenience and low background signal.

Generation and amplification of mouse PrP^{Sc} by interspecies PMCA

PrP^{Sc} of the hamster prion strain Sc237 was amplified by PMCA with mouse PrP^C substrate. Since the 4E10 antibody does not react with hamster PrP because of two amino acid substitutions in the epitope, it is possible to

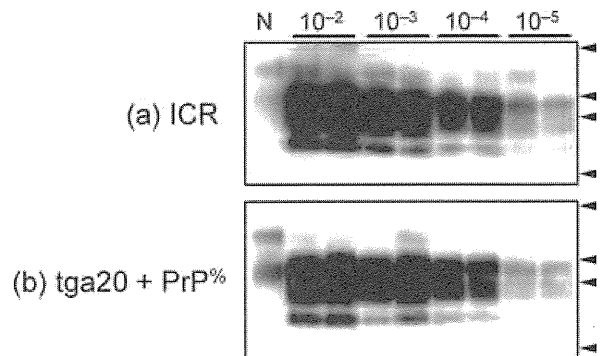


Fig. 1. Amplification of mouse-adapted Chandler scrapie PrP^{Sc} by PMCA. (a) PMCA was performed using ICR brain homogenate as the PrP^C substrates. Homogenates (10%) of Chandler-infected brains were diluted 1:100–1:100,000 with the PrP^C substrate. Amplification was performed in duplicate except for the negative control. (b) Amplification of Chandler PrP^{Sc} was performed using a mixture (1:5) of brain homogenates of tga20 and PrP^{0/0} mice as the PrP^C substrate. After PK digestion, the PMCA products were analyzed by WB using HRP-T2 monoclonal antibody. Arrows indicate the positions of molecular mass markers corresponding to 37, 25, 20, and 15kDa (Western C standards, Bio-Rad Laboratories, Hercules, CA, USA). N, control in which only PrP^C substrate was amplified.

determine the species from which PK-resistant PrP is derived. The generation of mouse PrP^{Sc} in the first round of amplification was clearly demonstrated by use of the 4E10 antibody (Fig. 2a). In the presence of digitonin, however, the PrP^{Sc} signal gradually decreased from the second to third round of amplification. Although addition of digitonin to the reaction mixture effectively reduces the background signal caused by aggregated PrP^C (PrP^{C-res}) in mice (17), digitonin might adversely affect interspecies amplification. The PrP^{Sc} molecules can be amplified by omitting digitonin from the amplification buffer (Fig. 2b,c), as described in the Materials and Methods section.

In contrast, the presence of the Sc237 seed was confirmed by 3F4 antibody in the first round amplification, and its remnant signal became lower than the minimum limit of detection in WB after the second round of amplification (Fig. 2a,b). PrP^{Sc} was detected by T2 antibody, which reacts with both mouse and hamster PrP after the fifth round of amplification (Fig. 2c). From the third to seventh rounds, the amplification efficiency was so low that the PrP^{Sc} could barely be maintained during the process of dilution of the PMCA products and its subsequent amplification. After this lag phase in amplification, the PrP^{Sc} signal became markedly intense. Although the spontaneous generation of PrP^{Sc} molecules has been reported previously (26, 27), no such PrP^{Sc} molecules were observed when the mouse PrP^C substrate alone was amplified by 10 rounds of serial PMCA (Fig. 2d). Therefore, the signal enhancement was caused by an increase in

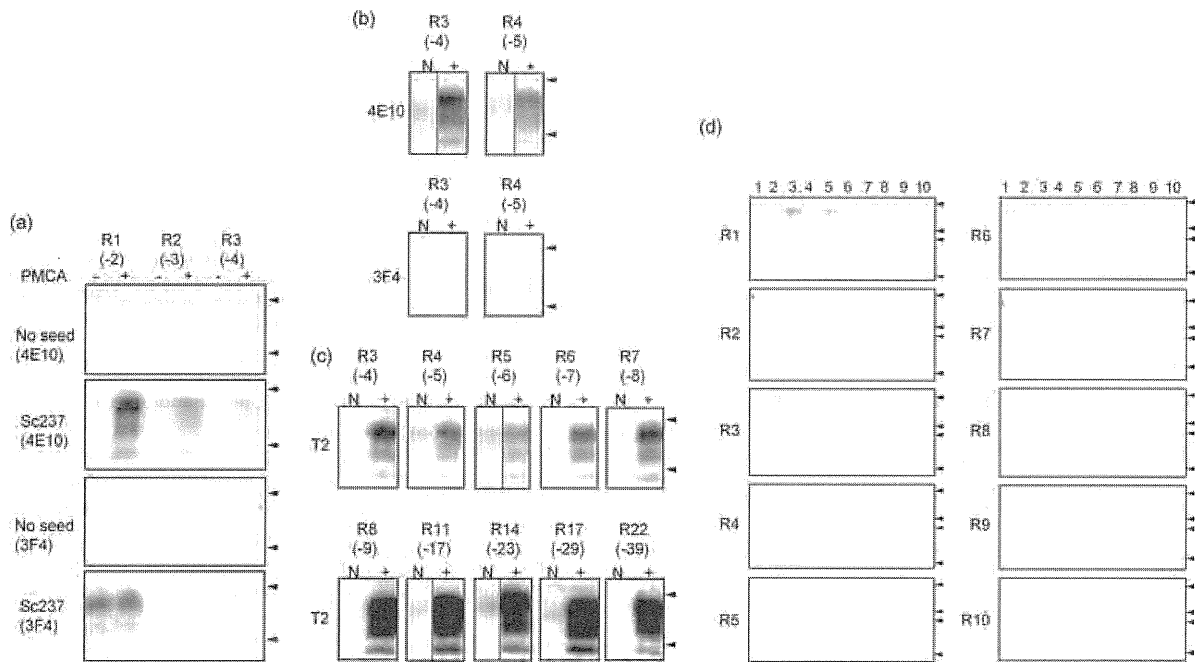


Fig. 2. Amplification of Sc237 hamster PrP^{Sc} by interspecies PMCA. (a) Hamster Sc237 PrP^{Sc} was amplified by serial PMCA with mouse PrP^C substrate. Amplification was performed in the presence of digitonin, and the R1–R3 samples were analyzed by WB with HRP-4E10 and AP-3F4 antibodies following PK digestion before (–) and after (+) amplification. Lanes labeled “No seed” represent the control reactions, which contained only the PrP^C substrate. Numerals in parentheses indicate the Sc237 seed dilution in each sample. Arrows indicate the positions of the 30 and 20kDa molecular mass markers (MagicMark XP, Invitrogen, Carlsbad, CA, USA). (b) The R2 product in Fig. 1a was amplified by serial PMCA in the absence of digitonin. The R3 and R4 products, labeled “+”, were analyzed by WB with HRP-4E10 and AP-3F4 antibodies following PK digestion. Lanes labeled “N” represent control reactions, these contained only the PrP^C substrate. (c) WB profiles of the R3–R22 PMCA products; PrP^{Sc} molecules were detected with HRP-T2 antibody. (d) No spontaneous generation of PrP^{Sc} was observed; samples 1–10 contained only mouse PrP^C substrate and were amplified in the absence of digitonin. The PMCA product was diluted 1:10, amplified, then diluted and amplified again for a total of 10 rounds. After each amplification round, samples (R1–R10) were analyzed by WB with HRP-T2 antibody after PK digestion. Arrows indicate the positions of molecular mass markers corresponding to 37, 25, 20, and 15kDa.

amplification efficiency after the eighth round of amplification. This high-efficiency amplification continued into the 22nd round of amplification, and a diglycosylated form of PrP^{Sc} molecules was predominant over other glycosylated forms throughout the amplification process.

Infectivity of Sc237 and interspecies PMCA-derived mouse PrP^{Sc} in tga20 mice

Table 1 shows the results of the bioassay. Contrary to what has previously been believed, the tga20 mice died after an average period of 548 ± 55 days when 10% brain homogenate of Sc237-infected hamsters was administered intracerebrally (Sc237/tga). The latent period in tga20 mice overexpressing mouse PrP^C was much longer than that in Tg52NSE mice with hamster PrP^C. Infectivity of the PMCA product from the 22nd round of amplification was also examined in these transgenic mice. Although

the control mice, which were inoculated with the homogenate diluted 1:800, had not developed the disease after more than 690 days, all tga20 mice inoculated with the R22 product (PMCA/tga) developed the disease after an average period of 345 ± 21 days. A significant difference was observed between the incubation periods of Sc237/tga and PMCA/tga mice. None of the Tg52NSE mice inoculated with the PMCA products developed the disease after more than 720 days.

Brain homogenates of the primary-passaged mice (Sc237/tga #1 and PMCA/tga #1) were injected intracerebrally into tga20 mice. In the secondary transmission, disease onset in the mice inoculated with brain homogenate of Sc237/tga #1 was significantly accelerated, and these mice (Sc237/tga-2) died after an average of 111 ± 2 days. In contrast, mice inoculated with brain homogenate of PMCA/tga #1 developed the disease after an average of 317 ± 6 days. There was no significant difference between

Table 1. Mean incubation time of tga20 and Tg52NSE transgenic mice

Inoculum (dilution of PrP ^{Sc} seed)		tga20				Tg52NSE	
		Primary passage		Secondary passage		Primary passage	
		Transmission rate (total death/total number)	Mean incubation time \pm SD (days)	Transmission rate (total death/total number)	Mean incubation time \pm SD (days)	Transmission rate (total death/total number)	Mean incubation time \pm SD (days)
Sc237	10 ⁰	100% (5/5)	548 \pm 55 ^{‡,§}	100% (4/4)	111 \pm 2 [§]	100% (5/5)	45 \pm 2
	8 \times 10 ^{-2†}	0% (0/5)	>690			100% (5/5)	61 \pm 1
Interspecies PMCA product	R22 (10 ⁻⁴⁰)	100% (5/5)	345 \pm 21 [‡]	100% (5/5)	317 \pm 6	0% (0/5)	>720

†, the 10% homogenates of Sc237-infected brains were diluted 1:800 and injected into transgenic mice as controls; ‡,§, the mice indicated by identical superscript symbols had significantly different ($P < 0.01$) mean incubation times.

the survival period of primary-passaged mice (PMCA/tga) and that of secondary-passaged mice (PMCA/tga-2).

Histopathological analysis of brains and spleens of tga20 mice inoculated with Sc237 and PMCA-derived mouse PrP^{Sc}

To characterize the neuropathological properties of Sc237 and the R22 PMCA-derived mouse PrP^{Sc}, we examined the regional profiles of neuronal vacuolation scores in the brains of affected mice ($n = 5$, Fig. 3). The vacuolation scores of mice inoculated with the PMCA-derived PrP^{Sc} were significantly different from those of mice inoculated

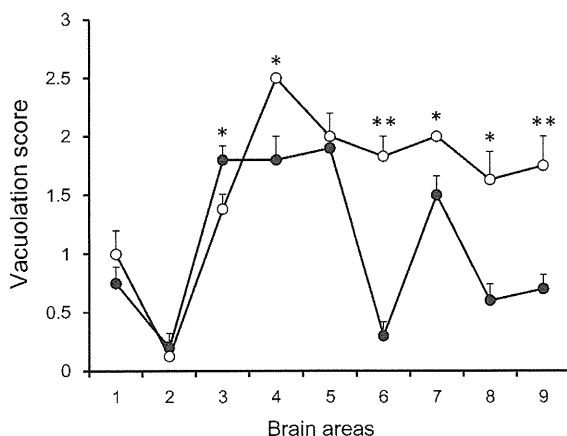


Fig. 3. Vacuolation profile in nine different brain areas of tga20 mice inoculated with Sc237 and PMCA. Brain regions are as follows: 1, dorsal medulla; 2, cerebellum; 3, midbrain; 4, hypothalamus; 5, thalamus; 6, hippocampus; 7, paraterminal body; 8, posterior midline of the cerebral cortex; 9, anterior midline of the cerebral cortex. The average lesion scores ($n = 5$ animals/group) and SEM (error bar) are shown in the graph. Asterisks denote significant differences between samples (two-tailed t -test, *, $P < 0.05$; **, $P < 0.001$). Closed circles, PMCA product; open circles, Sc237.

with Sc237 in six brain regions, namely the midbrain (region 3), hypothalamus (region 4), hippocampus (region 6), paraterminal body (region 7), posterior midline of the cerebral cortex (region 8), and anterior midline of the cerebral cortex (region 9). Furthermore, the vacuolation profiles of PMCA-PrP^{Sc} inoculated mice were distinct from those of mice inoculated with mouse scrapie strains such as Chandler, Obihiro, and 22A (unpublished observations). Immunohistochemical results from the brains and spleens of infected mice ($n = 5$) are shown in Fig. 4. In mice inoculated with Sc237, PrP^{Sc} accumulated over the whole region of the interpeduncular nucleus, midbrain, and medulla, diffuse distribution or synaptic-like immunostaining and plaque formation of PrP^{Sc} being observed in the corpus callosum. Although spongiform change was less frequent and PrP^{Sc} accumulation was not apparent in the brain sections of mice inoculated with the PMCA-derived mouse PrP^{Sc}, PrP^{Sc} deposition was observed in the spleens of these mice, as it was in the Sc237-inoculated mice.

Biochemical properties of PrP^{Sc} that accumulated in the brains of tga20 mice inoculated with Sc237 and the PMCA-derived mouse PrP^{Sc}

The WB profile of the PrP^{Sc} molecules that accumulated in the brains of tga20 mice inoculated with Sc237 (Sc237/tga) and the R22 PMCA products (PMCA/tga) was compared to the profiles of the Sc237 mouse scrapie prior strains (Obihiro, ME7 and Chandler), and the PrP^{Sc} generated by interspecies PMCA (R22 PMCA). The R22 PMCA PrP^{Sc} resembled the Sc237 rather than the mouse scrapie strains in the ratio of the three glycosylated forms of PrP^{Sc}, but the diglycosylated form of PrP^{Sc} was 0.7kDa smaller than that of the Sc237 PrP^{Sc} (Fig. 5a). The size of the unglycosylated PrP^{Sc} molecules of PMCA/tga #1 was 0.9kDa smaller than that of the Sc237/tga #1 mouse (Fig. 5a,b). This difference